arbitrary standard time of 48.0 hr. It was necessary to assume a value of λ_1 to obtain an approximate half-life and then make successive approximations. The corrected thulium activity is then, finally

$$A_{\mathrm{Tm}}(\mathrm{corr}) = A_{\mathrm{Tm}}(\mathrm{obs}) \frac{(e^{-\lambda_1 t_s} - e^{-\lambda_2 t_s})}{(e^{-\lambda_1 t} - e^{-\lambda_2 t})} \times \frac{1}{(\mathrm{Tm\ yield})\ (\mathrm{Er\ yield})},$$

where $A_{\mathrm{Tm}}(\mathrm{obs})$ is the activity extrapolated to the time of separation.

A plot was then made of the log of $A_{\mathrm{Tm}}(\mathrm{corr})$ *vs* the time to which the growth was corrected. A straight line resulted over a period of seven half-lives, as shown in Fig. 1. A least-squares analysis gave a value of 49.8 hr for the Er^{172} half-life. In consideration of the errors inherent in this milking technique, the probable error is set at ± 1 hr.

The β^- end-point energy of Tm^{172} was estimated by means of an Al absorption curve, giving a value of 1.5 Mev. The γ-ray spectrum was investigated by using a 50-channel pulse-height analyzer and a Tl-activated NaI crystal. Gamma rays of 1.79, 1.44, 1.09, and 0.076 Mev were found, in addition to the 0.049-Mev K x-ray. Two less prominent γ rays of 0.40 and 0.18 Mev were also noticed.

In addition the mass assignments of 10-hr Er^{165} and 7.5-hr Er^{171} were verified by a mass separation of 0.1% of the original erbium sample. The mass assignment of 1.9-yr Tm^{171} was also verified during the thulium run, by direct separation.

The authors wish to express their appreciation to the staff of the Materials Testing Reactor and of the 184-in. and 60-in. cyclotrons in Berkeley for their aid in making the irradiations.

PHYSICAL REVIEW VOLUME 103, NUMBER 1 JULY 1, 1956

Transient Nuclear Induction and Double Nuclear Resonance in Solids*

B. HERZOG AND E. L. HAHN†
Watson Scientific Computing Laboratory, International Business Machines, Columbia University, New York, New York
(Received December 7, 1955)

The behavior of transient nuclear induction signals from solids is described by a stochastic model based on a Markoff process. The model assumes the presence of local dipolar field fluctuations in a crystal due to a set B of coupled nuclei. These fluctuations can destroy or enhance the observed precessional coherence of a different set A of nuclei in the crystal. Coupling among A spins is assumed negligible. The spin echo of A formed at a given time t has an amplitude determined by the magnitude and rate R of field fluctuations. For values of Rt between zero and the order of unity the echo amplitude decreases, reaches a minimum at $Rt \sim 1$, and increases for $Rt > 1$. For R larger than the spin A static line width (when $R=0$) in units of frequency, line narrowing becomes effective, and is reflected in terms of increased lifetime and amplitudes of echo signals. The effect of B spin (Na^{23}) continuous wave resonance upon the echo relaxation of A (Cl^{35}) is studied in $NaClO_3$, a nuclear quadrupole system. For sufficiently weak cw rf excitation of Na^{23}, the behavior of Cl^{35} echoes roughly follows the behavior predicted by the stochastic model for changes in local field fluctuation rate R. The effect of coherent oscillations of local fields at larger cw rf excitation is discussed. Zeeman splittings of the Na^{23} quadrupole resonance are studied by the double resonance method. The decay of spin echo signals in liquids, as a result of molecular diffusion, is conveniently described by the stochastic model.

I. INTRODUCTION

RELAXATION times and line shapes in nuclear resonance experiments are often due primarily to one mechanism. In that case, with the analysis prescribed by one model, it is useful to determine how the nuclear relaxation should vary with changes in parameters of the system. We propose a model for the relaxation of free nuclear induction spin echo signals from nuclei which do not couple appreciably among themselves, but which lose spin precessional phase because of local magnetic field fluctuations caused by neighboring unlike spins in the crystalline lattice. The resulting transient signals are related to line shapes observed in steady state resonance. The properties of our specific model may be generalized qualitatively to apply to the general case of frequency fluctuations due to a variety of effects, and to account for observed effects due to double nuclear resonance in solids. From the point of view of signal transients our discussion includes some features of the statistical treatment of line shapes in solids by Anderson and Weiss[1] and Anderson.[2]

Let the observed relaxation of a collection of nuclei, denoted by A, be caused by dipolar field fluctuations at A which arise from neighboring unlike spins, denoted

* Submitted in partial fulfillment (by B. H.) of requirements for the degree of Doctor of Philosophy, in the Faculty of Pure Science, Columbia University.

† Present address: Physics Department, University of California, Berkeley, California.

[1] P. W. Anderson and P. R. Weiss, Revs. Modern Phys. **25**, 269 (1953).

[2] P. W. Anderson, J. Phys. Soc. Japan **9**, 316 (1954); R. Kubo and K. Tomita, J. Phys. Soc. Japan **9**, 888 (1954).

by B. Assume negligibly weak dipole-dipole coupling among the A spins and ascribe the dipolar field fluctuations experienced by the A spins to a continued reorientation of spins B because of (1) magnetic dipole coupling among B spins and (2) the forced magnetic resonance of the B spin system. The precessional frequency of A therefore suffers fluctuations due to the component of fluctuating magnetic field along the z axis of A spin quantization. Transverse dipolar fields of B acting on A in the xy plane are neglected as nonsecular perturbations, and the spin-lattice thermal relaxation times of A and B are assumed infinite. The effect of lattice motion on all spin-spin interactions is ignored. Double nuclear resonance is applied as follows: while the A spin resonance is observed directly, either in the steady state or by spin echoes, the B spins are simultaneously subjected to a continuous wave (cw) spin resonance. The modified local field fluctuations due to the forced resonance of B in turn vary the relaxation time for spin A precessional coherence. Thus A indicates the double resonance of B. If the coupling between A and B spins is sufficient, double resonance is readily detected and can be used to study this coupling. Moreover, it becomes possible to find extremely low-frequency nuclear resonances of the B system and to measure their line shapes by plotting changes in the relaxation of indicator nuclei A as the frequency of the oscillating field producing the B spin resonance is varied. Such low-frequency resonances occur when the direct magnetic dipole or electric quadrupole interaction of spin B is so small that the combination of an insufficient surplus spin population with a low transition frequency prohibits direct observation of the B resonance. Indirect observation of the B resonance requires sufficient coupling between systems A and B. Hence, the relaxation or line width of A and B should not be strongly determined by other processes such as line broadening due to paramagnetic impurities or short thermal relaxation times.

Double spin resonance experiments of different types have already been reported. Pound[3] first applied the double resonance method to excite different transitions of a given species of spin in order to study relaxation time effects. Overhauser, Slichter, and Carver[4] introduced the double magnetic spin resonance of different spins in order to enhance nuclear spin polarization by rf saturation of electron spins which couple with nuclei. Double resonance experiments in liquids by Royden and by Bloom and Shoolery[5] have demonstrated the coherent effect of forced reorientation of nuclear neighbors upon the indirect spin-spin interaction in organic molecules. In solids, where dipolar coupling is important, one would expect that the spin A line width would be markedly narrowed if the forced reorientation rate of spins B were large enough to average the local dipolar fields at spins A to a smaller value. This averaging effect is similar to the motional narrowing effect in liquids[6] and to the line narrowing obtained by the mechanical rotation of liquid samples in a fixed inhomogeneous external magnetic field carried out by Bloch and Arnold[7] and by Carr.[8] In order for mechanical rotation to be effective, the rotation rate must exceed the spread of Larmor frequencies due to the fixed inhomogeneity. Similarly, the double resonance line narrowing method in solids requires in our model that the reorientation rate of a majority of spins B exceed at least the spread in Larmor frequencies of spins A that exists in the absence of B resonance. In our experiments the spin echo envelope lifetime of A increases or decreases at the onset of the B resonance, depending upon the combined effects of internal coupling among the B spins and the intensity of the rf field applied for B resonance. For a large enough intensity of this rf field the spin echo envelope lifetime lengthens until the thermal relaxation time T_1 and the coupling among spins A became important in determining the echo decay. For T_1 infinite and no coupling among A spins, the echo envelope in our model should have an infinite lifetime in the limit of infinite reorientation rate of spins B since the free precession of spins A would no longer be perturbed by fluctuations of local fields which are then averaged to a zero value.

The change of nuclear polarization by the Overhauser effect[4] will not be important in our double resonance experiments to be discussed here for two reasons. First, the relaxation time for possible exchange of spin momentum between spins A and B is very long compared to observation times in which our signals last because of phase coherence; and second, spins B, upon rf saturation, will not have a sufficient Boltzmann population factor to provide a significant transfer of angular momentum to spins A.

A stochastic diffusion model is employed to obtain a qualitative prediction of the foregoing effects. We shall show that the fluctuations of magnetic fields at spins A can be followed qualitatively by use of standard probability functions well known in the theory of stochastic processes. A tracer technique, so to speak, is at our disposal to measure the transient behavior of the average field. The initial local field at spins A is prescribed by the steady state local field distribution (best approximated as Gaussian) at the time a first rf pulse initiates the free precession of A. At a later time, following a second (reversing) pulse, the A spins return a spin echo signal, which signifies a constructive interference of their macroscopic moment vectors. The diffusion model accounts for the manner in which the

[3] R. V. Pound, Phys. Rev. **79**, 685 (1950).
[4] A. Overhauser, Phys. Rev. **89**, 689 (1953); **92**, 477 (1953); T. R. Carver and C. P. Slichter, Phys. Rev. **92**, 212 (1953).
[5] V. Royden, Phys. Rev. **76**, 543 (1954); A. L. Bloom and J. N. Shoolery, Phys. Rev. **97**, 1261 (1955).
[6] Bloembergen, Pound, and Purcell, Phys. Rev. **71**, 466 (1947).
[7] F. Bloch, Phys. Rev. **94**, 496 (1954); W. A. Anderson and J. T. Arnold, Phys. Rev. **94**, 497 (1954).
[8] H. Y. Carr, Harvard thesis (unpublished).

individual spins that compose these moment vectors lose precessional phase as indicated by attenuation of the echo amplitude. Therefore, from echo measurements the average behavior of time varying local field fluctuations due to neighbors B can be inferred.

II. DIFFUSION CONCEPT OF LOCAL FIELDS

A treatment of field fluctuations in solids is logically preceded by a brief review of a similar effect upon the free precession of nuclear moments in liquids. Nuclear ensembles in low viscosity liquids, e.g., protons in water, have a natural line width of the order of one cycle per second. In order to resolve such narrow lines, the applied polarizing magnetic field H_0 must be sufficiently homogeneous so that the spatial variation ΔH of the field across the sample volume has a value $\Delta H \lesssim 1/(\gamma T_2)$, where γ is the nuclear gyromagnetic ratio and T_2 is the total relaxation time. If $\Delta H \gg 1/(\gamma T_2)$, the observed line width is determined by the field inhomogeneity ΔH. The double pulse echo method would allow a precise, independent measure of T_2 despite the unavoidable ΔH encountered in practice, if it were not for the Brownian motion of molecules in the liquid. This motion averages out the broadening due to neighboring dipolar fields, produces a longer T_2, but changes the Larmor frequency of nuclei by displacing them into the differing magnetic fields imposed by the fixed spatial field gradient dH/dx. The Brownian fluctuation of the position coordinate x produces a fluctuation in precessional phase, and the echo therefore attenuates in a time usually shorter than T_2.

From our treatment of field fluctuations in solids we shall present a reformulation of the spin diffusion theory in liquids in the appendix and correct some previous results. In former papers[9,10] a Larmor phase probability was used to describe the effect of self-diffusion in liquids upon the spin echo: moment vectors were assigned fixed initial frequencies which were to be remembered for certain time intervals while diffusion affected only the phase. In this paper we apply directly a probability distribution in Larmor frequency itself, which, after all, is the physical variable which fluctuates. When this is done, our results conform with those obtained by Carr and Purcell[11] and take into account the "refocusing effect" of diffusion discussed by them.

III. FORMULATION OF THE FREQUENCY DISTRIBUTION FOR SOLIDS

The notion of diffusion in the liquid case can be extended to solids. Local dipolar fields due to spins B now play the role of an inhomogeneous field ΔH_B formerly imposed by an external magnet. Initially we prefer to adhere to the A–B spin model set forth in the Introduction since the analysis for it allows some degree of rigor and the results are qualitatively useful. Later ΔH_B can be considered rather loosely as the equivalent local field at spin A from any combinations of (1) unlike neighboring nuclei, (2) neighboring electron spins, and (3) spin-spin coupling among spins A themselves. Nuclei A, which serve as an indicator of ΔH_B fluctuations, do not move through space. Instead, ΔH_B diffuses in the following sense: if ΔH_B increases at certain A sites in the crystal, there will be a corresponding decrease of ΔH_B at other A sites, or vice versa, in order to preserve the invariance of the instantaneous distribution of local field amplitudes seen by the A spins. The assumed distribution is the Gaussian

$$P(\delta_0)=\frac{1}{\delta_A(2\pi)^{\frac{1}{2}}}\exp[-\delta_0^2/(2\delta_A^2)], \tag{1}$$

where

$$\delta_0=\gamma_A\Delta H_B=\omega_0-\omega, \tag{2}$$

and

$$\int_{-\infty}^{\infty}P(\delta_0)d\delta_0=1. \quad \delta_A=\gamma_A\langle\Delta H_B\rangle_{\rm rms} \tag{3}$$

is the root-mean-square deviation in angular frequency, δ_0 is the frequency difference from exact spin resonance ω determined by a spin magnetic or quadrupole interaction, and ω_0 is the instantaneous precessional or transition frequency.

It is important to distinguish the role of $P(\delta_0)$ in our calculations from the distribution function or line shape which is actually measured in a resonance experiment. $P(\delta_0)$ expresses the *a priori* probability that a certain number of spins precess instantaneously at a frequency δ_0. This is nearly true in solids because at any instant of time the local field distribution will correspond roughly to the binomial distribution of a large number of B neighbor spin orientations. When ΔH_B becomes a random function of time, $P(\delta_0)$ is still the *a priori* weight function, but the measured line shape is determined by the time average of $\exp[-i\gamma_A\int\Delta H_B(t')dt']$, and will reduce to $P(\delta_0)$ only in the limit that ΔH_B is constant. Convenience dictates the choice of a Gaussian distribution function because the integrals that arise can be evaluated. Thorough discussion of these assumptions is presented in references 1 and 2.

The frequency deviation due to the dipole-dipole interaction between the ith A spin and N neighbors of type B is obtained from the Hamiltonian

$$\mathcal{H}=\gamma_A\gamma_B\hbar^2\mathbf{I}_{Ai}\cdot\sum_{j=1}^{N}\left\{\frac{\mathbf{I}_{Bj}}{r_{AiBj}^3}-\frac{3\mathbf{r}_{AiBj}(\mathbf{r}_{AiBj}\cdot\mathbf{I}_{Bj})}{r_{AiBj}^5}\right\}, \tag{4}$$

where I is the spin operator and r_{AiBj} is the distance between the ith A spin and the jth B spin. The line broadening of A is caused by the z component of field produced by B neighbors:

$$(\Delta H_B)_z=\delta_i(t)/\gamma_A,$$

[9] E. L. Hahn, Phys. Rev. **80**, 580 (1950).
[10] T. P. Das and A. K. Saha, Phys. Rev. **93**, 749 (1954).
[11] H. Y. Carr and E. M. Purcell, Phys. Rev. **94**, 630 (1954).

which appears at A. We define

$$\delta_i(t)=\gamma_A\gamma_B\hbar\sum_{j=1}^{N} m_{Bj}(t)G_{ij} \tag{5}$$

as the frequency deviation of the ith A spin, where

$$G_{ij}=(1-3\cos^2\theta_{AiBj})/r_{AiBj}^3,$$

θ_{AiBj} is the angle between $\mathbf{r}_{AiBj}$ and the z axis of quantization, and m_{Bj} is the magnetic quantum number of the jth B spin.

Let a number of spins, $S_\delta=nP(\delta)\Delta\delta$, out of all the n spins A in the crystal be characterized at any instant of time by the isochromatic frequency lying in the interval between δ and $\delta+\Delta\delta$, and let us explicitly examine how the configuration of all B nuclei produces this narrow range of δ. The symbol k shall now be used instead of i in (5) to distinguish those A spins which lie in this interval. For each of the S_δ nuclei A, (5) yields the relation

$$\delta_k=\gamma_A\gamma_B\hbar\{m_{B1}G_{k1}+m_{B2}G_{k2}+\cdots+m_{BN}G_{kN}\}, \tag{6}$$

where $k=1, 2, \cdots, S_\delta$. Due to crystalline symmetry it is possible for a certain number of B spins to have the same G factor, distinguished by a certain radius r and a certain $\cos^2\theta$. With this in mind, (6) is rewritten as

$$\delta_k=\gamma_A\gamma_B\hbar\{G_1(\sum_{s=1}^{s_1} m_{B1,s})_k+G_2(\sum_{s=1}^{s_2} m_{B2,s})_k+\cdots$$

$$+G_\rho(\sum_{s=1}^{s_\rho} m_{B\rho,s})_k+\cdots+G_P(\sum_{s=1}^{sP} m_{BP,s})_k\}. \tag{7}$$

The sum $\sum_{s=1}^{s_\rho} m_{B\rho,s}$, for example, means that all B spins having the same geometric factor G_ρ, namely s_ρ of them, are to be summed over fixed quantum numbers m which describe their individual spin states. The subscript k is dropped from the G factor, written in (6), and is used instead to distinguish the m values of those B spins in the configuration which produces δ_k. Now $G_1, G_2, \cdots, G_\rho, \cdots, G_P$ represent for any δ_k all the distinctive G factors which can apply. These factors are the same for each A spin in the periodic lattice, neglecting the correction due to crystalline boundaries. If all of the S_δ equations expressed by (7) are added together, the δ_k's sum to give $\bar{\delta}S_\delta$, where $\bar{\delta}$ corresponds to the average value in the interval between δ and $\delta+\Delta\delta$ for the local field spread which the set of S_δ spins A experience. This sum, in terms of the right-hand sum of (7) is

$$\bar{\delta}=[\gamma_A\sum_{\rho=1}^{P} G_\rho M_{\delta\rho}]/S_\delta, \tag{8}$$

where

$$M_{\delta\rho}=\gamma_B\hbar\sum_{k=1}^{S_\delta}(\sum_{s=1}^{s=s_\rho} m_{B\rho,s})_k$$

and $P\leqslant N$, depending upon the number P of different geometric factors G_ρ. We can define $M_{\delta\rho}$ as a sub-ensemble magnetic moment due to those B spins which (1) have the ρth geometric factor, and (2) contribute to local fields at spin A that see the average frequency $\bar{\delta}$. Of course a single B spin which contributes to $M_{\delta\rho}$ can at the same time be a member of other moments $M_{\delta'\rho}$ in other sets $S_{\delta'}$, and can also be a member of other moments $M_{\delta\rho'}$ within the same set S_δ. Therefore it is possible, in general, for a particular B nucleus to be a member, simultaneously, of macroscopic moments $M_{\delta\rho}$ which are distributed from positive to negative values. The separately labeled $M_{\delta\rho}$ moments, however, can be defined physically. The presence of an excess B spin population due to polarizing electric or magnetic fields is ignored here, since it would have negligible effect at normal temperatures. Actually in the definition of $M_{\delta\rho}$ the number of equivalent B spins (having the same G_ρ) contributing to $\bar{\delta}$ should be slightly less than $s_\rho S_\delta$, since a B spin can be counted more than once; namely, it can have the same G_ρ factor with respect to two or more A spins which happen to see the same $\bar{\delta}$. This correction is not of critical necessity. Even so, for small r_{AB}, first of all, it is unimportant for those values of line widths encountered in solids; and second, for large r_{AB} the correction would not modify the essential behavior of $\bar{\delta}$ since G_ρ is then negligibly small.

To give a stochastic treatment of ΔH_B or δ fluctuations we seek a law for the distribution of δ involving the time t. Now that δ has been expressed in terms of z components of B spin submacroscopic moments, we shall follow an $M_{\delta\rho}$ which is assumed to decay according to the classical equation

$$dM_{\delta\rho}/dt=-RM_{\delta\rho}, \tag{9}$$

so that

$$M_{\delta\rho}(t)=M_{\delta\rho}(0)e^{-Rt}, \tag{10}$$

where R is the decay rate. The average value $\bar{\delta}(t)$ seen by the same set of S_{δ_0} spins A at time t (define $\delta=\delta_0$ at $t=0$) is obtained by combining (8) and (10):

$$\bar{\delta}=\delta_0 e^{-Rt}. \tag{11}$$

At $t=0$ the relationship $\bar{\delta}=\bar{\delta}_0\approx\delta_0$ applies if $\Delta\delta_0$ is chosen arbitrarily small, so that all A spins in the set $S_{\delta=\delta_0}$ individually see nearly the same deviation δ_0. At a later time t, however, the actual δ seen by each of the A spins takes on a random value, but the average value $\bar{\delta}$ for all of them is still given by (11). The decay rate R is the same for all $M_{\delta\rho}$ moments, which means that all B spins have equivalent perturbing environments. Let

$$R=(1/T_B)+R_r, \tag{12}$$

where T_B is the natural time constant for decay of $M_{\delta\rho}$ due to mutual spin-spin flipping or exchange among the B spins. R_r, which will be defined explicitly later, describes an additional decay due to a weak applied double resonance rf field acting on B. Later our treatment will allow for higher intensity of double

resonance rf fields. For the present, let there be no double resonance and $R_r=0$.

The relaxation time T_B here plays a role similar to T_2, the transverse spin-spin relaxation time applied by Bloch[12] to M_x and M_y, but now $M_{\delta\rho}$ replaces $M_{x,y}$. Exchange of the z component of angular momentum occurs among different moments $M_{\delta\rho}$, but the total angular momentum of the B system, which is conserved, is zero. Mutual flipping among B spins belonging to the same $M_{\delta\rho}$ does not count as a relaxation process for that $M_{\delta\rho}$. At the same time, it is a relaxation process when the B spins are looked upon as members of different $M_{\delta\rho}$'s. Another interpretation may be attached to Eq. (9). Namely, T_B acts like the spin-lattice thermal relaxation time T_1 in the sense that a given $M_{\delta\rho}$ moment transfers magnetic energy and angular momentum to neighboring spins which are members of foreign $M_{\delta\rho}$ moments which can be of opposite sign. Hence, $M_{\delta\rho}$ does not arrive at a finite thermal equilibrium value M_0, as expressed by the well-known equation[12]

$$dM_z/dt=-(M_z-M_0)/T_1,$$

but becomes zero since M_0 is zero. Although M_0 for all the B spins may be finite, its effect at normal temperatures on the line width of spin A is negligible, as previously mentioned, and does not enter into our treatment.

It is necessary to find a function $P(\delta,t;\delta_0)\gtrless 0$ which is the probability that the frequency deviation of nucleus A is δ at time t if it had the value δ_0 at $t=0$. We want $P(\delta,t;\delta_0)$ to satisfy the following conditions:

$$\text{(I)}\qquad \int_{-\infty}^{\infty} P(\delta_0)P(\delta,t;\delta_0)d\delta_0=P(\delta), \tag{13}$$

where $P(\delta)$ is defined by Eq. (1) (there $\delta_0\rightarrow\delta$);

$$\text{(II)}\qquad \bar{\delta}=\int_{-\infty}^{\infty}\delta P(\delta,t;\delta_0)d\delta=\delta_0 e^{-Rt}, \tag{14}$$

which was obtained in (11); and furthermore

$$\text{(III)}\quad \int_{-\infty}^{\infty}P(\delta,t;\delta_0)d\delta=1,\quad \lim_{t\rightarrow\infty}P(\delta,t;\delta_0)=P(\delta), \tag{15}$$

with

$$\lim_{t\rightarrow 0}P(\delta,t;\delta_0)=0\quad\text{for}\quad\delta\neq\delta_0.$$

Condition (I) states that the instantaneous δ spectrum of spins A must be a stationary Gaussian distribution independent of the time. This is not to be confused with the measured spectrum, which is also independent of the time. Condition (II) establishes the relationship between $P(\delta,t;\delta_0)$ and the behavior of $M_{\delta\rho}$. All of the conditions above follow from the requirements of a random Markoff process. Thorough reviews of this process and related problems in diffusion are given by Uhlenbeck, Ornstein, Wang, Chandrasekhar, and Kac.[13] Conditions (I), (II), and (III) are uniquely satisfied by

$$P(\delta,t;\delta_0)=\left\{\frac{1}{\delta_A[2\pi(1-e^{-2Rt})]^{\frac{1}{2}}}\right\}\times\exp\left\{-\frac{(\delta-\delta_0e^{-Rt})^2}{2\delta_A^2(1-e^{-2Rt})}\right\}. \tag{16}$$

This solution for our model can be interpreted as the probability distribution which is obtained for δ if the stochastic differential equation

$$d\delta/dt+R\delta=F(t) \tag{17}$$

describes the variation of δ experienced by a single spin A. $F(t)$ is a fluctuating driving term, proportional to a fluctuating magnetic torque, assumed independent of δ and varying much more rapidly compared to the variations of δ. We can compare δ to the velocity u of a gas molecule of mass m, whose Brownian motion as a free particle is developed from the Langevin equation

$$du/dt+(f/m)u=A(t), \tag{18}$$

where f is the coefficient of friction and $mA(t)$ is a fluctuating force due to collisions. Uhlenbeck and Ornstein, and Chandrasekhar[13] show in detail how Eq. (18) leads to the distribution $P(\delta,t;\delta_0)$ if u is replaced by δ; f/m, by R; and $u_A^2=kT/m$, by δ_A^2. The stationary Maxwell-Boltzmann distribution of velocities is then the analog of the instantaneous frequency distribution $P(\delta_0)$ in our model.

IV. DAMPING OF THE FREE NUCLEAR PRECESSION FOLLOWING A PULSE

First let a short, intense rf pulse rotate the entire A spin macroscopic moment vector $\mathbf{M}_0$ by 90° into the xy plane. If the pulse width is t_w seconds and $\delta t_w\ll 1$, then the A spins retain precessional coherence during the pulse, and each of the component moments $\mathbf{M}_0P(\delta_0)$ are in phase at $t=t_w$ with an initial precessional frequency δ_0. A 90° pulse satisfies the condition $\gamma_A H_1 t_w=\pi/2$ where H_1 is the intensity of the effective rf field. The effect of field fluctuations upon the free precession of the A ensemble during the time $t\gtrsim t_w$ can be described if t is divided (let $t_w\ll t$) into K equal steps of short duration $\Delta t\ll 1/R$, where K is very large and $K\Delta t=t$. However, Δt is still so large that δ varies smoothly, but very little, while $F(t)$ in (17) undergoes many fluctuations. After the first time interval Δt the probability that those A spins, which form the moment $|F_0|=P(\delta_0)M_0$, arrive at a new frequency δ_1 is given

[12] F. Bloch, Phys. Rev. **70**, 460 (1946).

[13] G. E. Uhlenbeck and L. S. Ornstein, Phys. Rev. **36**, 823 (1930); M. C. Wang and G. E. Uhlenbeck, Revs. Modern Phys. **17**, 323 (1945); S. Chandrasekhar, Revs. Modern Phys. **15**, 1 (1943); M. Kac, Am. Math. Monthly **54**, 369 (1947). A convenient collection of these papers is in *Noise and Stochastic Processes*, edited by Nelson Wax (Dover Publications, New York, 1954).

by $P(\delta_1,\Delta t;\delta_0)$ from (16). During Δt, the average F_0 precession frequency is $\sim(\delta_0+\delta_1)/2$, but because of the large number of successive changes in frequency still to come, there will be little error in the final result from the assumption of δ_0 as the average frequency. The fraction $P(\delta_1,\Delta t;\delta_0)$ of each possible moment F_0 in the initial spectrum contributes a new moment, $|F_1|=P(\delta_1)M_0\phi$ having a frequency δ_1 at $t=\Delta t$, where the function $\phi<1$ contains a decay and phase factor which makes $F_1<F_0$ at the same position in the spectrum for which $\delta_1=\delta_0$. This is the result of phase fluctuations of nuclei which migrate out of initial frequencies δ_0 to the final specific frequency δ_1. The process is expressed by the integration

$$\begin{aligned}F_1&=iM_0\int_{-\infty}^{\infty}P(\delta_0)P(\delta_1,\Delta t;\delta_0)e^{i\delta_0\Delta t}d\delta_0\\&=iM_0P(\delta_1)\exp\{-\alpha(\Delta t)^2/4+i\delta_1\zeta\Delta t\},\end{aligned}\tag{19}$$

where $\zeta=e^{-R\Delta t}$ and $\alpha=2\delta_A{}^2(1-\zeta^2)$. The first term in the exponent of the factor ϕ accounts for the attenuation and the second term expresses the phase of the new moment F_1 at time Δt. The previous argument is repeated for succeeding time intervals. For example, during the next interval, between $t=\Delta t$ and $t=2\Delta t$, the distribution of moments F_1 contributes to a new moment F_2 at frequency δ_2. As time increases in steps Δt, $2\Delta t$, $\cdots$, $(K-1)\Delta t$, $K\Delta t$, the initial moments before each step are, respectively, F_0, F_1, $\cdots F_{K-2}$, F_{K-1} with respective frequencies δ_0, δ_1, $\cdots$, δ_{K-2}, δ_{K-1}. At time $t=K\Delta t$, the Kth moment is given by

$$F_K=\int_{-\infty}^{\infty}F_{K-1}P(\delta_K,\Delta t;\delta_{K-1})e^{i\delta_{K-1}\Delta t}d\delta_{K-1}.\tag{20}$$

F_{K-1} is obtained after $K-1$ integrations of this form in which $K\equiv1, 2, \cdots, K-1$. After these successive integrations,

$$\begin{aligned}F_K=\frac{iM_0}{\delta_A(2\pi)^{\frac{1}{2}}}\exp\{&-\delta_K{}^2/(2\delta_A{}^2)+i\Delta t\zeta\delta_K\sum_{l=0}^{K-1}\zeta^l\\&-\tfrac{1}{2}(\Delta t\delta_A)^2(1-\zeta^2)\sum_{j=0}^{K-1}(\sum_{l=0}^{j}\zeta^l)^2\}.\end{aligned}\tag{21}$$

Expressing the sums in close form, e.g.,

$$(1-\zeta^K)/(1-\zeta)=\sum_{l=0}^{K-1}\zeta^l,$$

and using relationships

$$t=K\Delta t,\quad \zeta^K=e^{-Rt},\quad R\Delta t\ll1,\quad \zeta\approx1-R\Delta t,$$

we find

$$\begin{aligned}F_K\approx\frac{iM_0}{\delta_A(2\pi)^{\frac{1}{2}}}\exp\{&-\delta_K{}^2/(2\delta_A{}^2)+i(\delta_K/R)(1-e^{-Rt})\\&-[\delta_A{}^2/(2R^2)][1+2Rt-(2-e^{-Rt})^2]\}.\end{aligned}\tag{22}$$

The observed transient nuclear induction signal T at time t following the 90° rf pulse is proportional to the sum of all precessing F_K moments in the spectrum, namely

$$T=\int_{-\infty}^{\infty}F_Kd\delta_K=M_0\exp\{-(\delta_A/R)^2(e^{-Rt}+Rt-1)\}.\tag{23}$$

Anderson[2] obtains (23) as the correlation function or Fourier integral corresponding to the line shape for a model which applies Markoff-Gaussian statistics.

V. SPIN ECHO

Before discussing the properties of T, the damping of spin echo signal E will be derived so that E and T can be compared. Let a second (180°) rf pulse be applied at $t=\tau$ under the conditions that held for the first pulse, except that $\gamma_AH_1t_w=\pi$. If τ is sufficiently large, the signal T will have attenuated to zero by the echo arrival time 2τ. It is then valid to assume that the first pulse is coherent with the second pulse, even though the two pulses are actually incoherent.[14]

Let u_A and v_A represent the real and imaginary components, respectively, of the A spin magnetization in a frame of reference rotating at the pulsed rf frequency ω; and let H_1 lie along the real axis in the direction of u_A for both pulses, which implies the coherence referred to above. Therefore, the complex magnetization at time τ is $F_K=(u_A)_K+i(v_A)_K$, given in (22). When a 180° pulse is applied at $t=\tau$, the component $(u_A)_K$ is unaffected, but $(v_A)_K$ is suddenly rotated by 180° about H_1 and transformed to $-(v_A)_K$. The analysis of free precession decay after $t=\tau+t_w$ thus starts with a moment $F_K{}^*$, analogous to $F_0=iM_0P(\delta_0)$ at $t=t_w$, where $F_K{}^*$ is the complex conjugate of F_K. Although the special case of a 90°–180° echo will be treated here, the results for attenuation of the echo E and the transient T are the same for any combination of tipping angles of the paired pulses. Only the over-all signal amplitudes will differ, depending upon constant factors involving trigiometric functions of $\gamma_AH_1t_w$. Successive integrations are again carried out, each of the type given by (20), and the initial moments prior to the time $(K+1)\Delta t$, $(K+2)\Delta t$, $\cdots$, $(L-1)\Delta t$, $L\Delta t$ are, respectively, $F_K{}^*$, F_{K+1}, $\cdots$, F_{L-1}, F_L. The frequencies δ again are distinguished by the corresponding time intervals. Note especially that the 180° pulse at $t=K\Delta t=\tau$ requires the integration

$$F_{K+1}=\int_{-\infty}^{\infty}F_K{}^*P(\delta_{K+1},\Delta t;\delta_K)e^{i\delta_K\Delta t}d\delta_K.$$

[14] Coherence is implied if rf oscillations of the second pulse are in phase with oscillations that are imagined to continue beyond the time oscillations actually cease beyond the first pulse. Double rf pulses in our experiments are incoherent since a self-excited oscillator is gated directly. Pulse coherence may be obtained by gating rf amplifiers which are preceded by a cw oscillator.

Using the relationships $K\Delta t=\tau$, $L\Delta t=t$, $\zeta^L=e^{-Rt}$ for $t>\tau+t_w$ and $T(\tau)\approx 0$, we find

$$F_L=\frac{iM_0}{\delta_A(2\pi)^{\frac{1}{2}}}\exp\{-\delta_L^2/(2\delta_A^2)+i(\delta_A/R)\times(e^{-R\tau}-e^{-R(t-\tau)})-[\delta_A^2/(2R^2)][2(\gamma\tau-1)+e^{-2\gamma\tau}\{2\gamma(t-\tau)-1\}+e^{-\gamma\tau}(4-e^{2\gamma\tau})]\}. \quad (24)$$

The observed echo signal E is obtained from the integration

$$E=\int_{-\infty}^{\infty}F_L d\delta_L=M_0\exp\{-(\delta_A/R)^2[R\tau-1+e^{-Rt}+R(t-\tau)e^{-2R\tau}]\}. \quad (25)$$

At $t=2\tau$ the echo signal has the maximum value

$$E_{\max}=M_0\exp\{-(\delta_A/R)^2[R\tau-1+(1+R\tau)e^{-2R\tau}]\}. \quad (26)$$

VI. PROPERTIES OF THE SIGNAL DAMPING

The transient T, Eq. (23), and the echo signal E, Eq. (25), behave as follows for the conditions indicated:

$R=0$:

$$T=M_0\exp\{-\delta_A^2t^2/2\};$$
$$E=M_0\exp\{-\delta_A^2(t-2\tau)^2/2\};\quad E_{\max}=M_0. \quad (27)$$

$Rt\ll 1$:

$$T\approx M_0\exp\{-\delta_A^2(t^2/2+Rt^3/6\};$$
$$E\approx M_0\exp-\delta_A^2\{(t-2\tau)^2/2+\tfrac{1}{6}R[12\tau^2(t-\tau)-t^3]\};$$
$$E_{\max}\approx M_0\exp(-2\delta_A^2R\tau^3/3). \quad (28)$$

$R=\infty$ (t and τ finite):

$$T=E=M_0. \quad (29)$$

$Rt,\ R\tau\gg 1$:

$$T\approx M_0\exp(-\delta_A^2t/R);$$
$$E_{\max}\approx M_0\exp(-\delta_A^2\tau/R). \quad (30)$$

In (27) $R=0$ implies that the local field ΔH_B is absolutely static. The signals then have the shape to be expected for free induction in an external inhomogeneous field with a Gaussian distribution, as predicted for liquids. For $R=\infty$ in (29), an infinite reorientation rate of spins B averages out the effect of ΔH_B, and the coherence of free precession is undisturbed. In (28), the condition $R\tau\ll 1$ is of interest in order to compare to the effect of self-diffusion in liquids, which is reviewed in the Appendix. In liquids the probability distribution used for the frequency is

$$P(\delta,t;\delta_0)=(2\pi Dt)^{-\frac{1}{2}}\exp\{-(\delta-\delta_0)^2/(4Dt)\}, \quad (31)$$

where D is the molecular self-diffusion coefficient of the spin-containing molecule. However (16) does not reduce to (31) in the limit $R\tau\ll 1$, letting $D=R\delta_A^2$, because of an extra term $\delta_0R\Delta t$ in the numerator expression of the exponent, which cannot be neglected in the Markoff analysis. Also, (31) does not obey the conditions expressed by (13) and (14), so that we would not expect the diffusion theory in liquids to be the limit of behavior of diffusion in solids for low D values or small τ. Yet in this limit the free induction signals in solids are characterized by decay terms in the exponent proportional to t^3 and τ^3, which also appear in the liquid theory.

The results in the limits $Rt,\ R\tau\gg 1$ in (30) are interesting since they confirm the result which Anderson and Weiss[1] obtain for rapid exchange of local fields, where the line shape in the stationary state becomes Lorentzian. Later it will be pointed out that this line shape corresponds to the ordinary exponential decay law of the induction transient, and the line narrows further or the transient lasts longer, as R becomes greater than δ_A^2t. Note that the time constant for the echo envelope decay is twice as large as the time constant for the decay of the free induction tail, since the echo occurs at $t=2\tau$. The echo formation in our model appears to involve a partial refocusing or reclustering of random spin vectors—an annulment of phase incoherence because of the phase reversal which follows the second pulse.[11] For the microscopic relaxation process pertaining to T_2 in liquids, this refocusing effect, if it did apply, would not be observed if $T_2\sim T_1$, since loss of signal due to T_1 cannot be recovered. But even for $T_1\gg T_2$ in liquids this refocusing effect does not occur because the local field fluctuations which nuclei experience are uncorrelated among themselves [Eq. (14) would not apply], whereas in solids there is such a correlation. In our model, where $T_1=\infty$, only (1) the spectrum intensity and (2) correlation of Larmor frequencies about zero frequency enter into the determination of spin echo signal decay. We have experimentally applied the Carr-Purcell technique[11] only to the case $Rt\ll 1$ in a solid, expecting to see some echo enhancement because of the train of 180° reversing pulses which follows a first 90° pulse. However, we observed no appreciable effect. We have not carried out the analysis to see how effective refocusing would be for the case $R\tau\ll 1$, but it appears that the Carr-Purcell method would be much more effective in the limit $R\tau\gg 1$, since many field fluctuations are necessary for the refocussing to be effective.

Plots proportional to the exponents in (23) and (26), shown in Fig. 1 are useful in studying the decay. The exponent in $T(t)$ is given by $A=(\delta_A/R)^2(e^{-Rt}+Rt-1)$, and in $E_{\max}$ it is given by

$$B=(\delta_A/R)^2[R\tau-1+(1+R\tau)e^{-2R\tau}].$$

In Fig. 1 the plots give

$$y_A=A(\delta_At)^{-2}=(e^x+x-1)x^{-2}$$

and

$$y_B=B(\delta_B\tau)^{-2}=[e^{-2x}(x+1)+x-1]x^{-2}$$

as a function of x for t and τ fixed, where we define

$x=Rt$ for y_A and $x=R\tau$ for y_B. The exponents in $T(\tau)$ and $E_{\max}(\tau)$ in (27), (28), (29), and (30) are confirmed by the plots in the various limits. $E_{\max}=e^{-y_B}$ is minimal when $x_{\min}=R\tau=1.35$ because y_B passes through a maximum at this point. This minimization is expected physically when the time 2τ necessary for the birth of an echo is of the order of the reorientation time $1/R$ of the perturbing local fields. If the conditions (*a*) $2\tau\gg 1/R$ or (*b*) $2\tau\ll 1/R$ apply, for the same τ above, the echo in comparison is much less attenuated. This follows because the fluctuation rate appears negligibly small in case (a), or the effect of many fluctuations averages nearly to zero in case (b).

Plots of $T(t)$ as a function of $s=t$ and $E_{\max}(\tau)$ as a function of $s=2\tau$ are given in Fig. 2 for different values of $P=(\delta_A/R)^2$. Throughout these plots a value of $\delta_A=2.94\times 10^3$ radians/sec is assumed as a typical rms value for chlorine quadrupole resonances observed in our experiments. The value of δ_A chosen is not particularly significant, but it is important to note how $T(t)$ and $E_{\max}(\tau)$, as functions of R and t or τ, confirm roughly the behavior of free nuclear precession in solids. We do not expect that the Cl quadrupole free precession in salts such as $NaClO_3$ and $p-C_6H_4Cl_2$ would be confirmed quantitatively by our $A-B$ spin model (Cl≡spin A; Na, H≡spin B). The theory is only useful in predicting the general behavior and orders of magnitudes of certain parameters in quadrupole systems. The $A-B$ spin model pertains to a purely magnetic interaction of spins with a common axis of quantization. The quadrupole chlorine-sodium or chlorine-hydrogen systems involve more than one axis of quantization, and the selection rules and energy states are somewhat different than those which occur in a purely magnetic coupled spin ensemble ($I=\frac{1}{2}$). Experiments in crystals involving magnetic coupling alone need to be carried out to confirm our theory more closely. Our approach to the diffusion problem was motivated by experiments in quadrupole resonance, where it was convenient to perform the double resonance, and for this reason the experimental results discussed in this paper are confined to measurements of quadrupole precession.

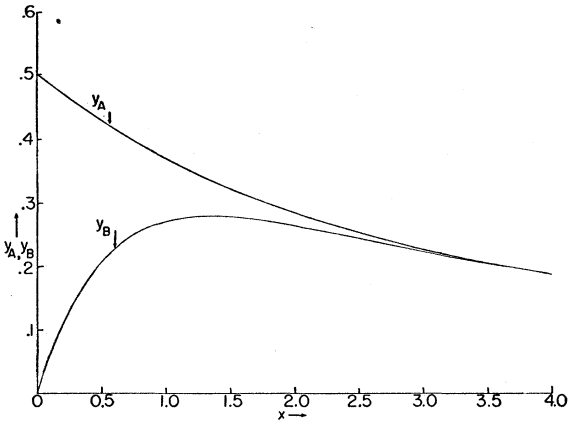

FIG. 1. Plots of exponents y_A and y_B of the functions $T(t)$ and $E_{\max}(\tau)$, respectively.

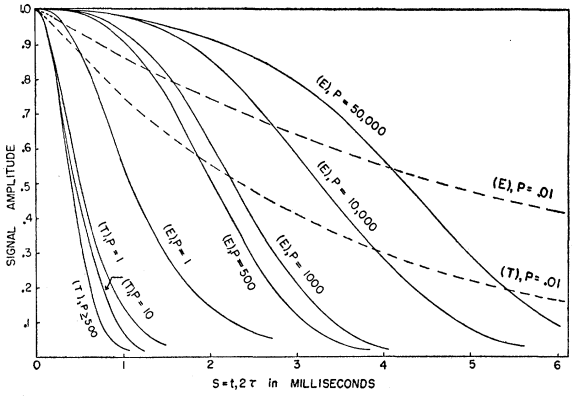

FIG. 2. Plots of free induction tails, T, and echo envelopes, E, for various values of the parameter $P=(\delta_A/R)^2$. The dotted lines plot nearly pure exponential decays for $P=0.01$, according to Eq. (30). The echo envelope lifetime is a minimum at $P\sim 1$, which is the condition at which true line narrowing becomes apparent (see Eq. (39)).

Figure 2 confirms several features of free precession observed in solids. Special effects, such as multiplet structure of the resonance, must be excluded. Empirically $T(t)$ and $E_{\max}(\tau)$ are observed to obey an $\exp\{-(t/T_2')^2\}$ law, where T_2' is a measure of the relaxation time. Although the $A-B$ spin theory does not specify a unique decay law, the theory fits this empirical law for t or τ in the theory not too close to the origin. The fit of $T(t)$ and $E_{\max}(\tau)$ to observed signals for all t and τ can be made rather good by adjusting R and δ_A. Another important feature is the fact that the echo envelope $E_{\max}(\tau)$ usually has a lifetime greater than the $T(t)$ signal. This is implied in Fig. 1, where exponents are plotted. For $R\tau$, $Rt\ll 1$ the echo amplitude is markedly larger than the induction tail. In systems of only like spins, $T(t)$ and $E_{\max}(\tau)$ have comparable lifetimes, where the echo is observable at 2τ when $\tau\sim 1/\delta_A$. Since the spins are the same, δ_A and $R=1/T_A$ are now closely related so that $\delta_A\sim R$ if we stretch our model to apply in this case. Consequently $R\tau\sim 1$, and $E_{\max}$ is close to its minimal value, as discussed previously, and its plot *versus* τ exhibits a short lifetime, nearer to a slightly shorter lifetime for $T(t)$.

In the $A-B$ spin system, if the B spin has a transition frequency determined by a quadrupole interaction, an internal change in R can be brought about by the application of a small magnetic field H_0. A Zeeman splitting of the zero field quadrupole levels occurs if $\gamma_B\hbar H_0\ll e^2qQ$, where e^2qQ is the quadrupole interaction. In $NaClO_3$, for example, $E_{\max}$ is quite close to its minimal value. With H_0 present, the relaxation time of Cl is always increased, because the Zeeman splitting of the Na quadrupole levels reduces fluctuations of ΔH_B. This occurs because a given Na nucleus in the field H_0 will couple less with Na neighbors distributed among

several Zeeman energy levels. The distribution in local fields at Cl sites is primarily due to Na neighbors, since the dipole interaction among Cl nuclei is negligible. The empirical lifetime T_2' of the echo envelope varies with the effective H_0 field as the $NaClO_3$ crystal orientation angle φ is varied with respect to the direction of a fixed external magnetic field. The reader is referred to a previous discussion[15] of this effect. It demonstrates how the reorientation parameter R, a complicated function of H_0 and φ, must vary in the $A-B$ spin model in order to account roughly for the observed $E_{\max}(\tau)$.

VII. CALCULATION FOR LINE SHAPE FROM THE INDUCTION TRANSIENT

Theorems presented by Anderson and Weiss[1,2] for line shape calculation can be applied and interpreted in terms of free precession to justify that the line shape is given by the Fourier transform

$$I(\eta)=\int_{-\infty}^{\infty} e^{i\eta\tau'}T(\tau')d\tau'. \tag{32}$$

Kubo and Tomita[2] obtain (32) in a rigorous fashion. Here η is the measured frequency deviation relative to the line center at ω, and $T(\tau')$ is given by Eq. (23) with $K\Delta t=\tau'$ instead of $K\Delta t=t$. We refer the reader to the above authors for further details concerning the theorems which we shall write down without proof as we apply them.

For a specific spectral line the spectrum of radiation or absorption of a quantum-mechanical system of spins can be written as

$$I(\eta)=\left|\int_{-\infty}^{\infty}\mu(t)e^{i\eta t}dt\right|^2, \tag{33}$$

where the matrix element of the dipole moment operator $S_x=\sum_j S_{xj}$ of j spins, summed over all states, gives

$$\mu(t)=\sum_{m,n}\langle m|S_x|n\rangle\exp\{-i(E_m-E_n)t/\hbar\}. \tag{34}$$

The sum is implied to be over only those energy levels m, n that satisfy the relation $E_m-E_n=\hbar\omega_0$ within the spectral line under consideration. It can also be shown that

$$\mu(t+\tau')=\mu(t)\exp\left\{-i\left[\omega_0(t+\tau')+\int_t^{t+\tau'}\delta(t')dt'\right]\right\}, \tag{35}$$

where $\delta(t')$ is identified with the fluctuating frequency referred to previously. This form of (35) has been previously used[9,10] in the analysis of the diffusion problem in liquids. Equations (33) and (35) combine to give

$$I(\eta)=\int_{-\infty}^{\infty}e^{i\eta\tau'}d\tau'\int_{-\infty}^{\infty}\exp\left\{-\int_t^{t+\tau'}\delta(t')dt'\right\}dt$$
$$=\int_{-\infty}^{\infty}e^{i\eta\tau'}\left\langle\exp\left\{-i\int_t^{t+\tau'}\delta(t')dt'\right\}\right\rangle_{\text{Av}}d\tau'.$$

It is convenient to let $\eta-\omega_0\rightarrow\eta$ since the line is described in terms of frequency differences from the line center. Anderson and Weiss attribute $\delta(t')$ to diagonal elements of the dipole-dipole Hamiltonian $\mathcal{H}$ given by (4), which change in a random manner because of external influences, such as the exchange narrowing effect in paramagnetic resonance. Our $A-B$ spin model specializes the effect of the diagonal element due to the z component of the local field ΔH_B from B spins. This viewpoint can now be generalized.

The transient signal $T(\tau')$ can be identified as an autocorrelation function

$$T(\tau')\propto\langle\mu(t)\mu^*(t+\tau')\rangle_{\text{Av}}$$
$$\propto\left\langle\exp\left\{-i\int_t^{t+\tau'}\delta(t')dt'\right\}\right\rangle_{\text{Av}}, \tag{36}$$

which represents the average of the memory of the precessional component $F_K(\tau')$ in (22) at $t+\tau'$ (let $t=0$) if it had the value $F_0(0)$ at time $\tau'=0$. F_K and F_0 are radiative macroscopic moments, proportional to the expectation values of S_x and, therefore to $\mu(t+\tau')$ or $\mu(t)$, respectively, expressed in Eqs. (34) and (35). It must be emphasized that the time $t+\tau'$, as it appears in (36), implies that the rf pulse is applied at $t=0$, and the free precession and correlation of moment vectors is measured as a function of τ'. Here we are applying an extension of the Wiener-Khintchine theorem to a nonstationary process.[16] Instead of averaging over all t in (36), we average over the ensemble frequencies beginning at the pulse time $t=0$. If the pulse width t_w is sufficiently short so that $\eta_{\text{Av}}t_w\ll1$, then all of the moment vectors are rotated by the same angle θ (which need not be just $\pi/2$) with respect to the z axis, and it is valid to state that $F_0=iM_0P(\delta_0)$ is proportional to $\mu(0)$ at $t=0$. If the pulse condition $\eta_{\text{Av}}t_w\gtrsim1$ exists, then only certain portions of the spin spectrum would be excited because of inadequate Fourier components in the pulse. Consequently the line shape $I(\eta)$ in (32) would not be truly represented because of distortion of $T(\tau')$ brought about, effectively, by "holes" in the summation over the m, n states in (34). In fact, for this case $I(\eta)$ would represent, in part, the Fourier spectrum of the pulse itself, and the result would be quite complicated.

The echo function E given by (25) represents a different type of autocorrelation than the function $T(\tau')$, and the question now is, what is the meaning of $I(\eta)$ in

[15] E. L. Hahn and B. Herzog, Phys. Rev. **93**, 639 (1954).

[16] D. G. Lampard, J. Appl. Phys. **25**, 802 (1954).

(32) if $T(\tau')$ is replaced by E? First consider $E=E_{\max}$. The envelope of $E_{\max}$ is plotted as a function of 2τ, and is a measure of the memory of refocusing or constructive interference of moment vectors. This memory is affected only by random frequency fluctuations and not by components of the local field which remain relatively static throughout $t=2\tau$. However, during the interval $\tau \rightarrow 2\tau$ there is some degree of cancellation of random phase accumulated in the first time interval τ. This is clearly seen in the experiment of Carr and Purcell where the influence of self-diffusion in liquids and gases is nearly eliminated by the application of a succession of 180° reversing pulses. It appears that if $E_{\max}$ were used as the correlation function in (32), then $I(\eta)$ would represent some sort of partial contribution to the actual line shape that pertains only to the effect of dynamic fluctuations of local field. The use of $T(\tau')$ in (32) permits $I(\eta)$ to include contributions from both static and dynamic effects on the local field which determine the true line shape.

It is more difficult to give a general physical interpretation of $I(\eta)$ if E is considered from the point of view of echo shape. Experiments in liquids indicate that the echo shape is made up of two tail signals $T(\tau')$ placed "back to back." However this is not generally true in our diffusion model, although it is nearly or actually true in certain limits of $R\tau$, as shown in (27), (28), (29), and (30). The echo shape is a function of times τ_1 before and τ_2 after the echo maximum time $t=2\tau$ if we replace t by $2\tau-\tau_1$ and $2\tau+\tau_2$, respectively, in (25). The "back to back" signals could be represented separately by the autocorrelation functions

$$E(\tau_1)=\langle F(2\tau-\tau_1)F^*(2\tau)\rangle_{\text{Av}}$$

and

$$E(\tau_2)=\langle F(2\tau)F^*(2\tau+\tau_2)\rangle_{\text{Av}},$$

where F is the precessing monochromatic magnetic moment at the instant of time noted.

From our model, in agreement with other authors,[2] we reasonably conclude that the entire measured line shape in steady state experiments would be determined by the integration

$$I(\eta)=\int_{-\infty}^{\infty}\exp[i\eta\tau'-(\delta_A/R)^2(e^{-R\tau'}+R\tau'-1)]d\tau', \quad (37)$$

where $T(t)=T(\tau')$ in (23) is introduced into (32). The line shape is of interest in the following limiting cases, referring to (28) and (30):

$R=0$ or $R\tau\ll 1$:

$$I(\eta)\approx M_0\exp\{-\eta^2/(2\delta_A^2)\} \quad (38)$$

which was originally assumed.

$R=\infty$:

$I(\eta)$ is a delta function, an infinitely sharp line.

$R\tau\gg 1$:

$$I(\eta)\approx\binom{2}{\pi}\frac{M_0\delta_A^2/R}{\eta^2+(\delta_A^2/R)^2}. \quad (39)$$

Anderson and Weiss have pointed out that the best model for the rough computation of line shapes and frequency moments is the Gaussian-Gaussian case, which is suitable for the description of exchange in paramagnetic resonance. Our $A-B$ spin model, based on a Markoffian-Gaussian process, requires that

$$\bar{\delta}=\delta_0 e^{-R\tau'}\propto\frac{\langle\delta(t)\delta(t+\tau')\rangle_{\text{Av}}}{\langle\delta^2\rangle_{\text{Av}}},$$

where the last term is the correlation function of the frequency. The Gaussian-Gaussian case[2] assumes that

$$\bar{\delta}=\delta_0\exp\{-\pi(R\tau')^2/4\}.$$

According to Anderson and Weiss for the latter case, the signal correlation function or transient induction would be given by

$$T(\tau')\sim\exp\left\{-\frac{\delta_A^2\tau'}{R}\int_0^{R\tau'}\exp\left(\frac{-\pi x^2}{4}\right)dx + [2\delta_A^2/(\pi R^2)][1-\exp(-\tfrac{1}{4}\pi\{R\tau'\}^2)]\right\}. \quad (40)$$

This also gives the same results for the limits discussed previously for the Markoff case.

If the behavior of $T(\tau')$ is deduced only in the limit of large or small τ', the limits $R\tau'\ll 1$ and $R\tau'\gg 1$ would be misleading in arriving at the approximate description of $T(\tau')$. Sampling the behavior near $\tau'=0$ would determine the shape of the wings of the line spectrum; and $T(\tau')$ for $\tau'\gg 0$ determines more correctly the shape near the center of the line. This can be understood from the fact that those precessing nuclei which first get out of phase see a large δ_0 and are situated in the wings of $P(\delta_0)$—these nuclei are the main cause of attenuation of $T(\tau')$ near $\tau'=0$. For $\tau'\gg 0$ they become completely out of phase and contribute little to $T(\tau')$. Then those spins with δ_0 nearer to zero begin to lose coherence and these are important in determining the shape of $T(\tau)'$.

VIII. EFFECT OF THE DOUBLE RESONANCE ON INDUCTION TRANSIENTS AND THE LINE WIDTH

In Eq. (12) an extra term R_r was included in R to account for additional random reorientation of B spins brought about by weak double resonance. From first-order perturbation theory,

$$R_r=W_B\gamma_B^2H_2^2T_{B0}, \quad (41)$$

where $1/T_{B0}$ is the rms value of the line width of spins B, H_2 is the magnitude of the double resonance perturbing rf field, and W_B is a resonance weight factor.

For a general double resonance treatment, however, it is not valid to introduce R_r in this manner. The Markoff diffusion model, as we have applied it in the absence of double resonance, implies that there are irreversible processes in which initial configurations of B spins never recur within an observation time. For arbitrary intensity of double resonance, however, the moment configurations $M_{\delta\rho}$ would oscillate in time. It is necessary, therefore, to modify the previous diffusion model in order to account for these oscillations, underdamped or overdamped, of $\delta(t)$ about a mean value, where the drift of the mean value is determined by irreversible processes. We shall invoke the diffusion model for the bound oscillator which is treated by Ornstein and Uhlenbeck and reviewed by Chandrasekhar.[13] First the macroscopic behavior of $M_{\delta\rho}$ is treated at exact resonance using the Bloch equations,[12] out of which an average $\bar{\delta}$ is obtained for the same purpose that $\bar{\delta}$ in (11) was obtained in the case for no double resonance. A new probability function $P(\delta,t;\delta_0)$ is then obtained and applied to calculate the free induction transients T and E, again by the Markoff method.

The submacroscopic moment $M_{\delta\rho}$ is described in the frame of reference rotating at ω_2, the applied double resonance frequency. We now write M_B in place of $M_{\delta\rho}$. Transverse components of magnetization u_B and v_B, defined earlier in the case of A spins, become associated with M_B because of the presence of H_2. The macroscopic equations of motion are assumed to be

$$dv_B/dt-u_B\Delta\omega+\omega_2 M_B=-v_B/T_{B0}, \tag{42}$$

$$du_B/dt+v_B\Delta\omega=-u_B/T_{B0}, \tag{43}$$

$$dM_B/dt-v_B\omega_2=-M_B/T_B, \tag{44}$$

where $\Delta\omega=\omega_{0,B}-\omega_B$ is the deviation from the resonance center, T_{B0} is the transverse or total relaxation time of the B spins, T_B is the relaxation time corresponding to the natural reorientation rate defined previously, and $\omega_2=\gamma_B H_2$. We assume that T_B and T_{B0} are unaffected by H_2, particularly if H_2 is weak. For $\Delta\omega=0$ the differential equation for M_B is

$$d^2M_B/dt^2+\beta(dM_B/dt)+\alpha M_B=0, \tag{45}$$

where

$$\beta=(1/T_B)+(1/T_{B0}), \quad \alpha=\omega_2^2+(T_BT_{B0})^{-1}.$$

The solution of (45) is

$$M_B(t)=M_B(0)e^{-\beta t/2}\left[\cosh\left(\frac{\beta_1 t}{2}\right)+\left(\frac{\beta}{\beta_1}\right)\sinh\left(\frac{\beta_1 t}{2}\right)\right]$$
$$-\frac{2}{\beta_1}\frac{dM_B(0)}{dt}e^{-\beta t/2}\sinh\left(\frac{\beta_1 t}{2}\right), \tag{46}$$

where

$$\beta_1=[\{(1/T_B)-(1/T_{B0})\}^2-4\omega_2^2]^{\frac{1}{2}}.$$

As written, $M_B(t)$ expresses the case for overdamping where β_1 is real. For the periodic case β_1 is imaginary and for critical damping β_1 is zero. Inserting (46) into (8) gives the average value.

$$\bar{\delta}=\delta_0 e^{-\beta t/2}\left[\cosh\left(\frac{\beta_1 t}{2}\right)+\frac{\beta}{\beta_1}\sinh\left(\frac{\beta_1 t}{2}\right)\right]$$
$$-\frac{2\dot{\delta}_0}{\beta_1}e^{-\beta t/2}\sinh\left(\frac{\beta_1 t}{2}\right). \tag{47}$$

The appearance of the derivative $\dot{\delta}_0$ here leads to the question whether, for a given initial frequency δ_0, there is a distribution in δ_0. For such a general treatment it is necessary to evaluate integrals of the type

$$\int_{-\infty}^{\infty}\int_{-\infty}^{\infty}P(\delta_0)P(\dot{\delta}_0)P(\delta,\Delta t;\delta_0,\dot{\delta}_0)$$
$$\times P(\dot{\delta},\Delta t;\dot{\delta}_0,\delta_0)e^{i\delta_0\Delta t}d\delta_0 d\dot{\delta}_0 \tag{48}$$

for the Markoff step analogous to (19). The probabilities $P(\delta,\Delta t;\delta_0,\dot{\delta}_0)$ and $P(\dot{\delta},\Delta t;\dot{\delta}_0,\delta_0)$ must be determined so that they are jointly consistent with conditions (13), (14), (15), using the average values of δ and $\dot{\delta}$ obtained from (8).

Our experimental quadrupole data does not warrant such an involved treatment using (48) so its application shall be deferred and presented in a later paper. Instead, we find it is sufficient to assume that $\dot{\delta}_0$ in (47) is correlated in a definite way with δ_0, such that

$$\dot{\delta}_0=C\delta_0, \tag{49}$$

where C is a constant involving ω_2, T_B, and T_{B0}. In this way it becomes possible to predict the rough behavior of double resonance for rf fields H_2 not too large, such that

$$\omega_2\lesssim\tfrac{1}{2}\{(1/T_{B0})-(1T_B)\}=1/2T^*. \tag{50}$$

$1/T^*$ is defined as the static contribution to the line width of B spins, or the spread in Larmor frequencies due to spatial variations in local fields along the z axis. The constant C is determined by requiring at $t=0$ that $\dot{M}_B(0)=CM_B(0)$ and at $t=\Delta t$ that $\dot{M}_B(\Delta t)=CM_B(\Delta t)$. Applying these conditions to (46), and using (8), we find $C=-(\beta+\beta_1)/2$. Evidently (50) must apply, or M_B, which is a real quantity, could become imaginary.

The transient functions $T(t)$ and $E(\tau)$ for double resonance will have the same form as (23) and (25), respectively, repeating steps beginning with (19), except that now $R=(\beta+\beta_1)/2=-C$ replaces $R=1/T_B$, and δ_A^2 must be modified. Consider the behavior of R in the limit $\omega_2T^*\ll 1$. We would expect $R\rightarrow\{(1/T_B)+\omega_2^2T_{B0}\}$, where $\omega_2^2T_{B0}$ compares to $R_r=W_B\omega_2^2T_{B0}$ defined in (41). Instead, as a property of our model, $R\rightarrow\{(1/T_B)+\omega_2^2T^*\}$ is the proper limit. In spite of this, it will be convenient later to use R_r in place of $\omega_2^2T^*$ for purposes of qualitative discussion of double resonance in $NaClO_3$, particularly since $T_{B0}\sim T^*$.

Now the question of modification of the *a priori* spin

spectrum by double resonance must be considered. In the absence of B spin-spin coupling, the double resonance field H_2 at resonance ($\Delta\omega=0$) must create a new stationary distribution of moments $v_B\neq 0$ and M_B, which results in the reduction of $\delta_A{}^2$ to a lower value $\delta_A{}'^2$. The moment M_B ($\omega_2=0$), defined in the absence of double resonance, can be thought of as being tipped slightly when $\omega_2\neq 0$, so that M_B makes an angle θ with respect to the z axis. Therefore

$$\cos\theta\,|_{T_B=\infty}=M_B(\omega_2=0)/[M_B{}^2(\omega_2\neq 0)+v_B{}^2(\omega_2\neq 0)]^{\frac{1}{2}}.$$

When the entire ensemble is averaged, then

$$\delta_A{}'^2=\delta_A{}^2\cos^2\theta. \tag{51}$$

Using the fact that

$$\dot{M}_B=-\tfrac{1}{2}(\beta+\beta_1)M_B \quad (\text{at } T_B=\infty)$$

together with (44), one finds

$$\cos^2\theta=\frac{2\omega_2{}^2T^{*2}}{1-(1-4\omega_2{}^2T^{*2})^{\frac{1}{2}}},$$

where

$$4\omega_2{}^2T^{*2}\leqslant 1 \quad \text{or} \quad \theta\leqslant\pi/4.$$

The transient induction signals with double resonance are now written as

$$T(t)=M_0\exp\left\{-\left(\frac{2\delta_A{}'}{\beta+\beta_1}\right)^2 \times[e^{-(\beta+\beta_1)t/2}+(\beta+\beta_1)t/2-1]\right\} \tag{52}$$

and

$$E(\tau)=M_0\exp\left[-\left(\frac{2\delta_A{}'}{\beta+\beta_1}\right)^2\{(\beta+\beta_1)\tau/2 -1+[1+(\beta+\beta_1)\tau/2]e^{-(\beta+\beta_1)\tau}\}\right], \tag{53}$$

where $\delta_A{}'^2$ is given by (51). Using (53) we obtain curves

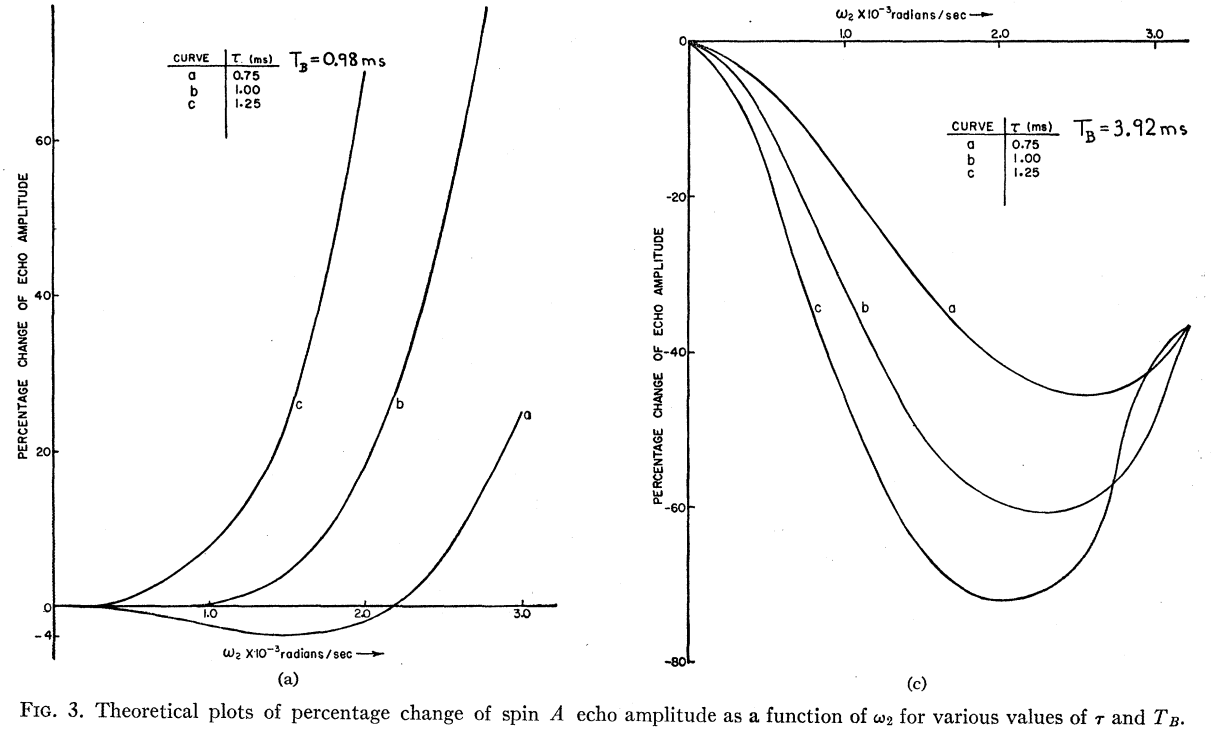

FIG. 3. Theoretical plots of percentage change of spin A echo amplitude as a function of ω_2 for various values of τ and T_B.

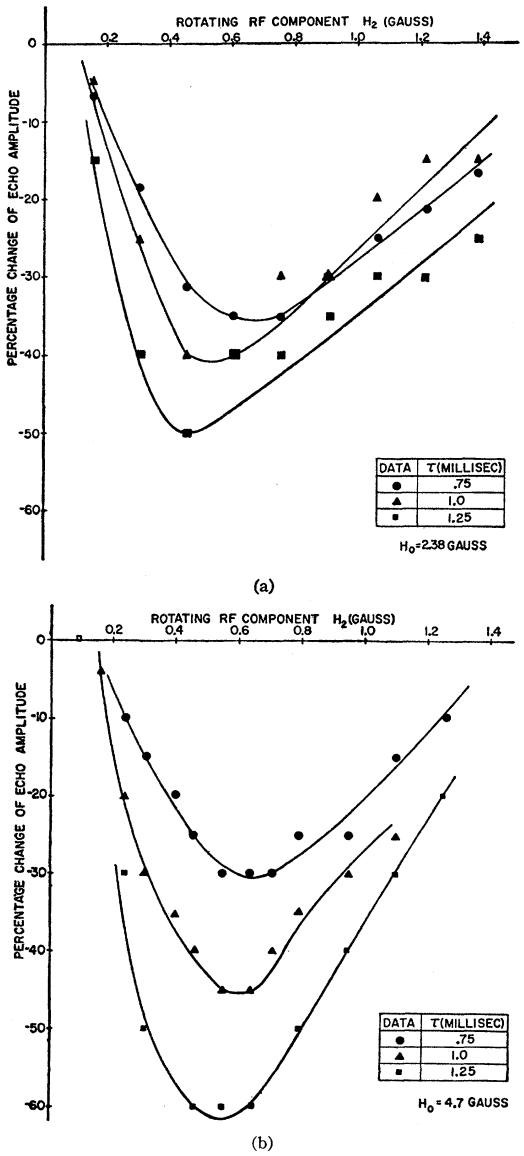

FIG. 4. Experimental plots of percentage change of Cl^{35} echo amplitude in $NaClO_3$ as a function of the cw rf field $H_2=\omega_2/\gamma_{Na}$ applied to obtain Na^{23} quadrupole resonance. The increase in T_B with H_0 inferred from these curves corresponds roughly with the trend indicated by the theoretical curves in Figs. 3(b) and 3(c). The value of $1/T^*$ for the inverse line width of the B spins in the theory was not chosen particularly to correspond with $1/T^*$ of Na^{23} in $NaClO_3$.

in Figs. 3(a), 3(b), and 3(c) which plot the theoretical percent echo amplitude change,

$$\frac{E_{\max}(\omega_2=0)-E_{\max}(\omega_2=\omega_2)}{E_{\max}(\omega_2=0)}\times 100,$$

for fixed values of $\tau=0.75$, 1.00, and 1.25 milliseconds. Each of the figures plots curves for $1/T_B$ fixed at $1/T_B'$, $1/2T_B'$, and $1/4T_B'$, where $1/T_B'=1.02\times10^3$ sec^{-1}. For all the curves $1/T^*=7.2\times10^3$ sec^{-1} and $\delta_A=2.94\times10^3$ rad/sec. These numbers were chosen as a rough approximation to the parameters involved in the double resonance in $NaClO_3$ of Na^{23} (spin B) with $\gamma_B=7.24\times10^3$ and Cl^{35} (spin A) with $\gamma_A=2.62\times10^3$. The number for $1/T^*$ is particularly arbitrary, since it assumes a virtual spread of $\Delta H_B=1$ gauss for the Na line. This value includes the effect of quadrupole broadening in our experiments because of thermal gradients over our samples. Actually $\Delta H_{\text{rms}}=0.44$ gauss is the computed value due to nuclear Na neighbors alone.

The curves compare qualitatively with experimental plots of Cl echoes obtained in $NaClO_3$, as shown in Figs. 4(a) and 4(b). The limitations in making a comparison to a quadrupole system are discussed in the next section.

Line narrowing by double resonance occurs if the reorientation rate R of local fields is rapid compared to the inverse of the observation time $t=\tau'$ of nuclear precession. When $T(t)$ expressed by (52) is integrated in (32) to obtain $I(\eta)$, an expression identical with (42) is obtained for $R\tau'\gg1$, except that $\delta_A\rightarrow\delta_A'$ and

$$R\rightarrow(1/T_B)+(1/2T^*)[1-(1-4\omega_2{}^2T^{*2})^{\frac{1}{2}}].$$

Narrowing becomes effective when

$$\delta_A'\lesssim(1/T_B)+(1/2T^*)[1-(1-4\omega_2{}^2T^{*2})^{\frac{1}{2}}],$$

insofar as our limited theory is concerned, where $2\omega_2T^*\leqslant1$. In this range δ_A' varies from δ_A to $\delta_A/2$. As one would expect, the breadth of the B spin spectrum, $1/T^*$, must not be excessive if H_2 is to be effective in flipping a sufficient number of spins. If there is an appreciable spin flipping rate $1/T_A$ among the A spins, ω_2 would have to be larger in order to affect the line width, and would not have as much influence in determining the line width. We have not considered $1/T_A$ in our treatment but it may be included crudely by adding $1/T_A$ to $1/T_B$ in Eq. (44), so that narrowing becomes effective when

$$\delta_A'\lesssim(1/2T_A)+(1/T_B)+(1/2T^*)-\tfrac{1}{2}[\{(1/T_A)+(1/T^*)\}^2-4\omega_2{}^2]^{\frac{1}{2}}.$$

The addition of $1/T_A$ in this way is essentially a transformation in which the A spins appear not to couple, but the B spins virtually have a larger reorientation rate by the amount $1/T_A$. Redfield[17] and Abell and Knight[18] obtain narrow lines in solids with increases in rf fields, before rf saturation broadening sets in, where only one species of nucleus is subjected to cw resonance. In terms of our model, these experiments may be considered as though the A and B spins are identical, serving both as indicator nuclei and sources of field fluctuations. There is the added complication, of course, of spin-spin coupling among the indicator nuclei. Also it should be emphasized that we have neglected any dependence of T_B and T_{B0} on H_2, which would be particularly im-

[17] A. G. Redfield, Phys. Rev. **98**, 1787 (1955).
[18] D. F. Abell and W. D. Knight, Phys. Rev. **93**, 940 (1954).

portant for H_2 large, as indicated by Redfield.[17] This dependence should arise for reasons which account for the change of relaxation of the A spins.

Figures 5(a), 5(b), and 5(c) show echo signals from Cl^{35} in $NaClO_3$ as they pass through a minimum with increasing values of H_2 applied at the Na resonance. Figure 6 indicates the variation of the echo amplitude, for fixed τ and given values of $(\delta_A\tau)^2$, as a function of $x=R\tau$. The dotted line shows how the echo amplitude varies with application of the double resonance field H_2, where the initial echo amplitude is determined by $R\tau$ at $H_2=0$.

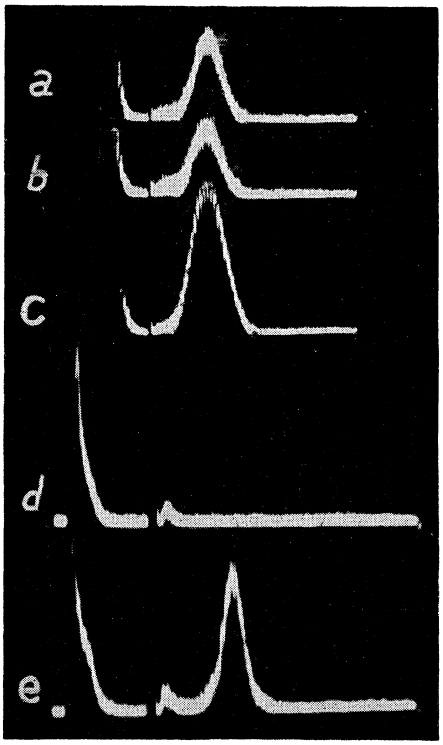

FIG. 5. Oscilloscopic displays of double resonance effect upon Cl^{35} echo amplitude. Trace a shows the normal echo ($H_2=0$) in $NaClO_3$ with $2\tau=2.25$ msec and $H_0=25$ gauss along lattice cell edge. Traces b and c display amplitude changes due to Na^{23} resonance at 395.1 kc/sec (X resonance) for $H_2=0.3$ g and 1.0 g, respectively. Trace d shows the echo in $p-C_6H_4Cl_2$ completely attenuated at $2\tau=3.4$ msec with $H_0=19.9$ g. Resonance of a portion of the proton spectrum with $H_2=6.7$ g at 88.9 kc/sec in e lengthens the echo lifetime radically.

IX. EXPERIMENTAL PROCEDURE AND RESULTS

Apparatus

The extension from single to double resonance is rather simple: a second coil C forming part of a tuned circuit and driven through an amplifier by a calibrated oscillator is placed around the sample to produce the second magnetic field H_2 (see Fig. 7). If the double resonance is nuclear magnetic, the usual geometric arrangement of coil axis perpendicular to orienting magnetic field H_0 must exist.

As before, the spin echo is observed directly on the

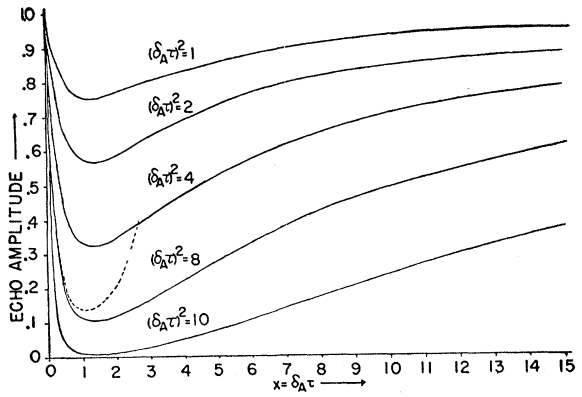

FIG. 6. Theoretical plots of echo amplitude variation. The solid curves are plots of Eq. (26) with $H_2=0$ for different values of $(\delta_A\tau)^2$. For τ fixed at 1 millisecond and $(\delta_A\tau)^2=8$, the single dotted curve shows the echo amplitude variation as R increases with increase in H_2. R is then replaced by $(1/\beta)+(1/\beta_1)$, and Eq. (53) is used to obtain the plot. "The abscissa '$x=\delta_A\tau$' should read $x=R\tau$."

oscilloscope, but now the natural signal amplitude when $H_0=0$ is compared with its height for various values of H_2. The presentation has been facilitated by switching H_2 on and off electronically at the end of alternate triggered sweeps at a slow repetition rate. This assures equilibrium for the H_2 resonance exists when rf pulsing starts near the beginning of sweeps. Large amplitude variations are thus graphically portrayed, but slight changes within the noise region on the signal are obscured due to screen persistence. The alternation presentation has been used mainly for qualitative indication of resonance. Photographic display without alternation is preferable for quantitative study. Finer details of amplitude changes may be observed with the "box car" integrating system.[19]

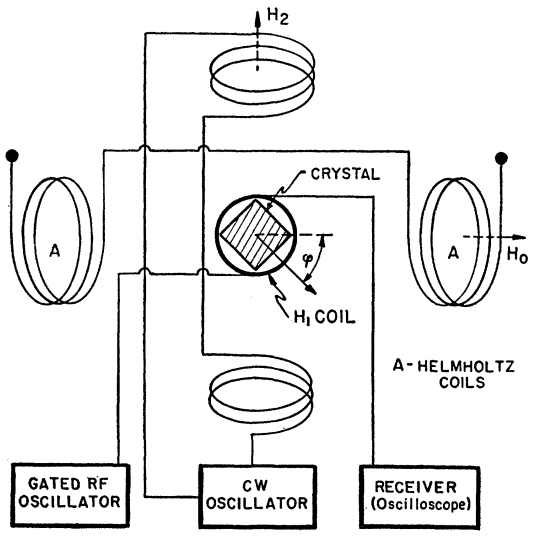

FIG. 7. Experimental arrangement for obtaining double resonance.

[19] R. E. Norberg and D. F. Holcomb, Phys. Rev. **98**, 1074 (1955).

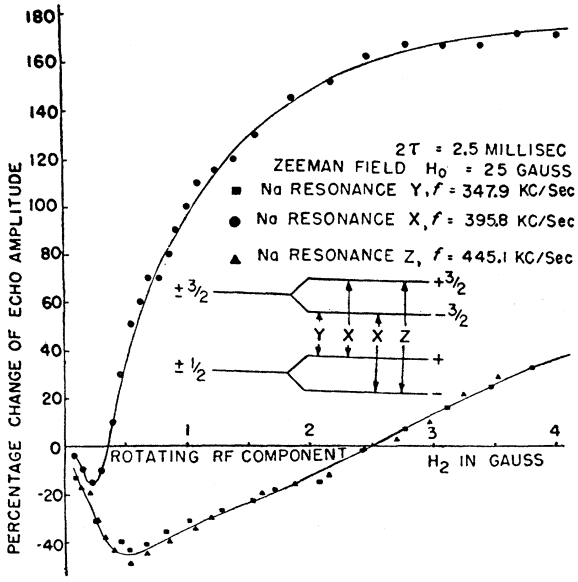

FIG. 8. Effect of Na^{23} resonance upon Cl^{35} echo in a single $NaClO_3$ crystal. The magnetic field H_0 is perpendicular to the 100 plane.

The magnitude of the linearly polarized field $2H_2$ at the sample site was measured with a nonresonant pickup loop of known parameters inserted into the double resonance coil which was tuned to resonance for various driving frequencies. No more than a maximum H_2 of $\sim$5 gauss at 400 kc/sec could be applied because of interference due to 30-Mc/sec harmonics from the 400-kc/sec power amplifier which overloaded the high-frequency receiver. These harmonics interfered with the chlorine echoes observed at about 30 Mc/sec.

Double Nuclear Quadrupole Resonance

Earlier measurements indicated that neighboring sodium nuclei in $NaClO_3$ are the main contributors to Cl^{35} echo decay. In an attempt to simulate the effect of Zeeman decoupling discussed in Sec. VI, the double resonance of Na^{23} was performed at a frequency of 400 kc/sec corresponding to the axially symmetric pure quadrupole interaction.[20] The cw rf field H_2 increases the reorientation rate R of Na beyond its value $1/T_B$ established by internal spin-spin coupling alone in the presence of H_0. Figure 8 shows the percentage change of echo amplitude as a function of H_2 for a fixed H_0 field and rf pulse spacing τ. A $NaClO_3$ single crystal orientation with the 100 plane perpendicular to H_0 is chosen to provide Zeeman level spacings which allow three resonances for either nucleus, each of spin $I=3/2$. Throughout the time that all three Cl transitions are excited by short rf pulses and the Cl echoes are observed at $\sim$30 Mc/sec, the cw resonance of a single Na transition (X, Y, or Z) is carried out. When the Na resonance corresponding to X is excited, the rf transition rate is calculated to be four times the rate for transitions Y or Z. This follows for transitions between pure $\psi_{+3/2}$, $\psi_{-3/2}$ states and the mixed states

$$\phi_+ = (2/3)^{1/2}\psi_{+1/2} + (1/3)^{1/2}\psi_{-1/2}$$

and

$$\phi_- = (1/3)^{1/2}\psi_{+1/2} - (2/3)^{1/2}\psi_{-1/2}$$

for this specific crystal orientation. Although our classical theory cannot apply in all respects to quadrupole systems, it at least confirms the order of magnitude in the difference of depths and positions of the minima in Fig. 8. This is seen by replacing ω_2^2 by $W_B\omega_2^2$ in Eq. (53). Neglecting a slow dependence of δ_A' on H_2 for the sake of simplicity, Eq. (53) then passes through a minimum for $(\beta+\beta_1)\tau/2\sim 1$, as shown before in Eq. (26) for $R\tau\sim 1$. Since τ is the same for both plots, then we expect to have $R_X \approx R_{Y,Z}$ at the minimum of the X and Y, Z curves, respectively. From our foregoing assumptions, the ratio

$$W_{B,X}/W_{B,Y,Z} = H_{2,X}^2(\min)/H_{2,Y,Z}^2(\min) = 4$$

should apply. A ratio of 4 is observed as seen in Fig. 8.

The difference in the depth of each of the minima results from the fact that the reduction factor $\cos^2\theta$ introduced in (51) applies to a different fraction of B spins when X is excited than when Y or Z is excited. The matrix elements for the various transitions serve as weighting functions so that $\delta_A^2\cos^2\theta_X$ should be replaced by $\delta_A^2(2\cos^2\theta_X+1)/3 = U_X$ for the two simultaneous transitions, and $\delta_A^2\cos^2\theta_{Y,Z}$ should be replaced by $\delta_A^2(\cos^2\theta_{Y,Z}+5)/6 = U_{Y,Z}$ for the Y or Z transition. Since $U_X < U_{Y,Z}$, then (53) will behave such that the X minimum is not as deep as the Y, Z minimum, and the echo signal increase for the X resonance is much faster with increasing H_2.

The plots of percentage echo amplitude changes in Figs. 4(a) and 4(b) were made with cw excitation of either the Z or the Y resonance of Na. In the theoretical plots of Fig. 3(a), (b), and (c), $\delta_A^2\cos^2\theta_{Y,Z}$ was not replaced by $\delta_A^2(\cos^2\theta_{Y,Z}+5)/6$, nor was $W_{Y,Z}(\sim 1)$ introduced. However, these changes would not seriously alter the qualitative confirmation of relative positions of curve depths and minima shown by the experimental curves.

By means of double resonance, the Zeeman splitting of the Na^{23} quadrupole transition in a small magnetic field H_0 was traced as a function of crystal orientation (Fig. 9). The measured spectrum agrees well with the first-order perturbation theoretical values[21] for the eight possible resonances. In units of $\gamma H_0/(2\pi\sqrt{2})$, the frequency separations from the zero field transition are given by $\pm\Delta f$, where $\Delta f = \sqrt{3}(\cos\rho)(2-\cos^2\rho)^{\frac{1}{2}}$ and ρ can assume the values $\varphi \pm \pi/4$. Further details regarding the Zeeman splitting and crystal orientation angles φ are given in a previous discussion.[15]

[20] J. Itoh and R. Kusaka, J. Phys. Soc. Japan **9**, 434 (1954).

[21] R. Livingston, Science **118**, 61 (1953); Ting, Manring, and Williams, Phys. Rev. **92**, 1581 (1953).

Figure 10 plots the Cl echo amplitude as a function of the applied double resonance frequency which traces through the triplet Na resonances indicated in Fig. 8. The percentage increase or decrease of amplitude maxima of the outer lines (Y, Z transitions) and central line (X transition) relate to the plots in Fig. 8.

An important reason for not expecting complete agreement between our theory for a system of pure magnetic coupling and the experiment in $NaClO_3$ lies in the fact that complete reversal in space of the $M_{\delta\rho}$ submacroscopic moments is not caused by H_2. A nuclear quadrupole moment undergoing resonance can only shuttle back and forth among either the positive or negative angular momentum states, but not among both. For this reason the Cl free precession lifetime of induction signal $T(t)$ could be increased only slightly by intense values of H_2 applied to Na, nor could the echo shape be changed appreciably. Although the local field fluctuations due to Na can be averaged to a lower value, double resonance cannot reduce a static field distribution which remains when the Na nuclei are locked in directions of either positive or negative angular momenta that do not easily interchange. This separate grouping of spin states can be broken down, however, by transitions between the mixed Zeeman states ϕ_+ and ϕ_-. These transitions can be induced either by internal fluctuating fields or an externally applied field. Itoh[20] has observed the transition directly by an absorption experiment, which must of necessity rely upon a sufficient Boltzmann population excess of spins. We have observed this transition at $\nu=16$ kc/sec indirectly via double resonance in a weak Zeeman field ($H_0\sim 8$ gauss) oriented according to the conditions discussed for Fig. 8. The resonance condition is

$$\nu=(1/2\pi)\sqrt{3}\gamma_{\mathrm{Na}}H_0.$$

The spin population difference then was negligible and unimportant here; yet the indicator Cl echo amplitude was markedly decreased by the forced shuttling of Na between the two states, causing strong variations in Na—Cl dipolar coupling. Echo enhancement was not observed.

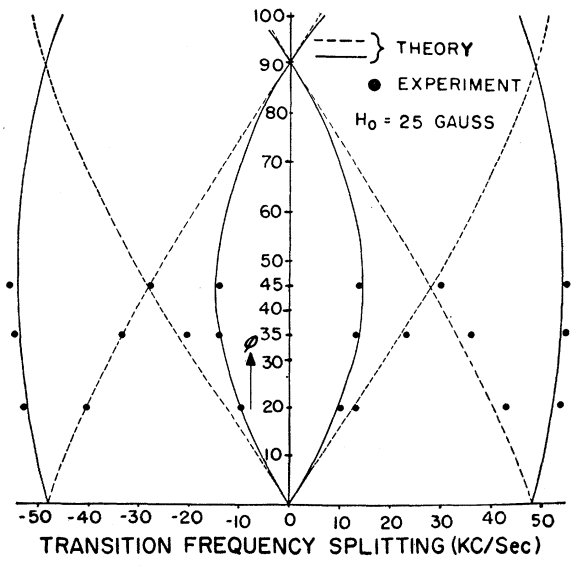

FIG. 9. Zeeman splitting of Na^{23} quadrupole levels in $NaClO_3$, measured from observation of maximum changes of chlorine echo amplitudes. (Zero-field frequency = 396 kc/sec.)

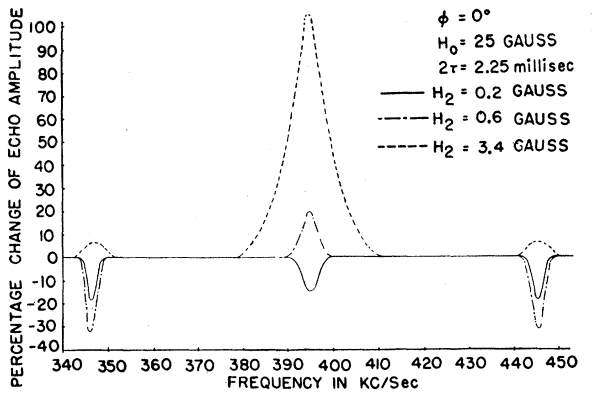

FIG. 10. Percentage change in Cl^{35} echo amplitude as a function of rf frequency applied to obtain Na^{23} resonance in $NaClO_3$. The Zeeman spectrum of Na^{23} is plotted out in accordance with the transitions and conditions indicated in Fig. 8. For increasing amplitude of H_2 the resonance radiation broadening of the Na^{23} resonance is reflected in terms of a broad response in the chlorine echo amplitude.

In the absence of a small magnetic field H_0 it was difficult to affect the chlorine echo lifetime by resonance of Na at ~400 kc/sec. We attribute this to the fact that transitions at a much lower frequency occur between mixed Zeeman states ϕ_+ and ϕ_- which arise from magnetic dipole-dipole coupling among Na nuclei. It would be necessary to obtain a Na resonance not only at 400 kc/sec, but also simultaneously at a low frequency $\sim 1/T^*$ before the chlorine echo can be enhanced. With H_0 applied such that $\gamma_{\mathrm{Na}}H_0 \gg 1/T^*$, then the $\phi_+ \rightleftarrows \phi_-$ transitions due to internal Na—Na coupling is markedly reduced, and only the 400-kc/sec resonance is sufficient to influence the chlorine echo.

A similar study of the Na^{23} double resonance at 400 kc/sec has been made in $NaBrO_3$, which has a lattice isomorphic with $NaClO_3$. Echo amplitude changes for Br^{81} at 150 Mc/sec are quite similar to those previously described.

Nuclear Magnetic-Nuclear Quadrupolar Double Resonance

The chlorine quadrupole interaction in *para*-dichlorobenzene has already been examined[22] and proven most useful in studying crystalline phase transitions. Free induction measurements at room temperature of the pure quadrupole transition for Cl^{35} at ~34 Mc/sec

[22] C. Dean and R. V. Pound, J. Chem. Phys. **20**, 195 (1952).

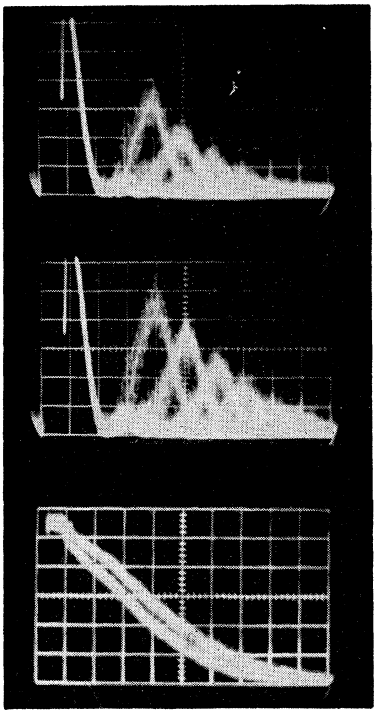

FIG. 11. Zero external magnetic field double resonance of protons in p-dichlorobenzene as it affects the free precession of Cl^{35}. The upper trace of the chlorine echo envelope is given for no double resonance ($H_2=0$). Assuming an $\exp[-(t/T_2')^2]$ echo envelope lifetime dependence, $T_2'=0.95$ msec. In the middle oscillographic trace all the conditions are the same except that protons are subjected to double resonance at 11.6 kc/sec with $H_2=2.3$ gauss. T_2' increases to 1.11 msec. The sweep speed for these two traces is 220 μsec/cm division. The lower traces indicate the free precession chlorine signal after the first pulse. A double exposure indicates first an induction signal lifetime of $T_2=0.3$ msec for $H_2=0$ gauss and then a lifetime $T_2=0.4$ msec for $H_2=2.3$ gauss.

show that the signal $T(t)$ has a lifetime $\sim$0.5 sec, the spin echo $E(\tau)$ signal has a lifetime $\sim$0.95 msec, and $T_1\sim$18.5 msec. The echo lifetime is rather insensitive to the lengthening effect[15] of a small applied magnetic field because the mutual flipping rate among the protons providing the local field variations is hardly reduced by H_0. No new frequencies are introduced, whereas H_0 produces new levels in a quadrupole system ($I>1/2$). This field, in conjunction with local dipolar fields, establishes the magnetic resonance frequency of the protons.

Because a B-spin system with $I=1/2$ should agree better with theory developed so far, the double resonance of the protons was performed. A large increase, but never a decrease, of echo amplitude under proton double resonance is observed in Fig. 5(d), (e). This is contrasted with the Cl echo in $NaClO_3$ which passes through a minimum. This fact implies that the proton mutual flipping rate is already larger than the echo-minimization value, and $(\beta+\beta_1)\tau\gg1$ applies in Eq. (52). Our search of the proton spectrum in this way shows a complicated multiplet structure due to configurations of proton neighbors. Since only a narrow section of the proton spectrum can undergo resonance at one time for a moderately weak H_2, a large number of the protons continues to flip at the "natural" rate, and the echo lifetime cannot be increased to the T_1 of Cl^{35} even though in principle T_1 is the upper limit if the dipolar coupling among Cl^{35} nuclei can be neglected. Furthermore, in such low-frequency resonance the observed spectrum may not be symmetric about an H_0 field which is comparable to the local fields and hence sufficiently weak to have the splitting extend to negative frequency values. A "fold-over" effect then takes place in which the usually neglected oppositely rotating component of the linearly polarized rf field H_2 can cause transitions and add to the spectrum by its double resonance effect upon the indicator echo. Because of these complications no attempt was made to compare the observed signals to theory, except in a qualitative way.

The zero-field transitions of protons at frequencies established by the average value of their mutual local fields alone[23] is also observable by double resonance, without the requirement of a net proton spin population. The echo amplitude increase was so slight, however, that a thermal gradient[24,25] had to be produced in the crystal to permit echo observation unimpeded by decaying tail signals after narrowly spaced pulses. This artificial broadening of the quadrupole levels led to a shorter T_2 but did not affect the echo lifetime in p-$C_6H_4Cl_2$, thus confirming that the protons provide the echo relaxation mechanism. In Fig. 11 the echo relaxation was observed to lengthen from 0.95 msec to 1.11 msec with $H_2=2.3$ gauss at 11.6 kc/sec, where the main peak of the proton zero-field spectrum appeared to be.

Sources of Error

Lack of temperature control of the samples during the measurements explains some of the deviations from theory since the quadrupole interaction is temperature dependent. For example, the experimental error of the Zeeman spectrum data (Fig. 9) should include the shift of the central resonant frequency as the temperature changed slightly. The existence of thermal gradients over the crystals can be particularly pernicious when one relates the effect of double quadrupole resonance to increasing H_2 values since the static line with $1/T^*$ plays an important role in the theoretical description. Quantitative agreement between Fig. 8 and Fig. 10 therefore cannot be expected because the measurements were made when "thermal equilibrium," or the same T^* due to thermal gradients if any, was assumed to have been reached.

Slight misalignments of the crystals in H_0 could not be avoided. When crystalline orientations were known

[23] F. Reif and E. M. Purcell, Phys. Rev. **91**, 631 (1953).
[24] M. Bloom, Phys. Rev. **94**, 1396 (1954).
[25] Bloom, Hahn, and Herzog, Phys. Rev. **97**, 1699 (1955).

from other information, the echo modulation pattern (Fig. 4 of reference 15) itself served to determine the angular setting $\varphi=0°$ for $NaClO_3$, for example.

For large values of H_0 ($\gtrsim 15$ gauss) the various chlorine transitions were not equally excited by the rf pulses because it was difficult to satisfy the required conditions $1/t_w \ll \gamma_{Cl} H_0$ and $\gamma_{Cl} H_1 t_w \sim \pi/2$. These conditions insure that there are sufficient Fourier components in the rf pulses to excite all of the chlorine Zeeman levels, and to obtain sufficient echo amplitudes. Unequal excitation of the X, Y, and Z resonances, for example, of the chlorine Zeeman spectrum (similar to that of Na, since Cl has spin $I=3/2$) also introduces a certain complication. In a quadrupole system, terms like $e^{iA\delta(t)}$ should be averaged instead of $e^{i\delta(t)}$ [see (19)], where A is a constant factor different for the various transitions but of the same order of magnitude.[25] These terms arise from computation of the Zeeman effect. We make no attempt to include this in our theory. Such a complication does not prevent $NaClO_3$ from displaying at least the qualitative aspects of our theory, which applies only to a purely magnetic coupled system.

X. CONCLUDING REMARKS

A statistical model for the precession of spins in solids has been presented under the following main assumptions; (a) collections of nuclei specified by an average Larmor frequency obey classical nuclear induction equations; (b) fluctuations of local fields are followed by the Markoff process, using standard probability functions associated with this process; (c) indicator nuclei do not couple with each other. Although observed effects in quadrupole systems have been presented as a justification for our model, which applies to a purely magnetically coupled system, these effects are very similar to those which occur in solids where spins undergo pure magnetic resonance. Investigations are being continued in systems of purely magnetically coupled spins to check our model more closely, and to complete measurements which will show what happens in the limit of extremely intense rf fields applied to the B spins. Equation (48) must then be introduced into the calculations instead of (19) in order to account generally for the effect of double resonance, and to avoid certain artificial assumptions. Although the assumption of correlation between δ_0 and $\dot{\delta}_0$ (Eq. 49) allows a limited description in the region of small rf fields H_2, it cannot be generally correct. It leads to such a solution for $T(t)$, that the second moment of the line shape is given by

$$\left.\frac{d^2T(t)}{dt^2}\right|_{t=0} = \int_{-\infty}^{\infty} I(\eta)\eta^2 d\eta = \delta_A{}'^2,$$

where $T(t)$ is given by Eq. (23) and $\delta_A{}'^2$ is given by Eq. (51). Here the second moment $\delta_A{}'^2$ is not invariant with respect to H_2, which it should be,[26] just as the second moment is invariant with respect to any exchange type effect.[1,2]

The property that the echo amplitude passes through a minimum for $R\tau\sim 1$, or that the echo envelope lifetime passes through a minimum for increasing R (see Fig. 3), should be considered in the measurement of what is thought to be the usual relaxation time, or inverse line width $1/T_2$. In general the echo envelope is not a true measure of T_2 except in the limit that we deal only with liquids of sufficiently low viscosity where the local magnetic fields fluctuate sufficiently rapidly and where there is no crystalline structure which would impose a correlation among these fluctuations. Explicitly by correlation it is meant that it would not be possible to define an average local field $\bar{\delta}=\delta_0 \exp(-Rt)$ as deduced in Eq. (11). This is not to be confused with the correlation function introduced by Bloembergen, Pound, and Purcell,[6] where they show in liquids that essentially $\langle\delta^2\rangle_{Av} e^{-t/\tau_c}$ applies, where τ_c is effectively the time between molecular collisions. From echo envelope measurements Holcomb and Norberg[19] infer that the inverse line width $1/T_2$ decreases at the melting points of Li and Na metals. It is reasonable to expect that the fluctuation rate R of local fields due to diffusing nuclear neighbors will satisfy the condition $R\tau\sim 1$ or $\delta_A/R\sim 1$ as the temperature is increased. In order to account for this effect our echo relaxation theory would have to be modified to include correlations both in δ and in $\langle\delta^2\rangle_{Av}$. Thus, assuming T_2 to be a true measure of echo envelope lifetime, T_2 would pass through a minimum. A true measure of T_2 would be obtained from a measurement of $T(t)$, Eq. (23), or from a line shape measurement, after correcting for any external field inhomogeneity.

ACKNOWLEDGMENTS

We thank Professor L. Brillouin and Professor C. H. Townes for stimulating discussions. We thank Mr. R. J. Blume, Mr. W. V. Kiselewsky, and Mr. W. P. Jones for their able assistance in the construction of the apparatus. We are indebted to Dr. A. L. Schawlow of the Bell Telephone Laboratories for providing us with single $NaClO_3$ and $NaBrO_3$ crystals.

APPENDIX

Consider the effect upon spin precession of the self-diffusion of molecules in liquids. Let the solution to the diffusion equation for a free particle apply:

$$P(x,\Delta t) = (4\pi D\Delta t)^{-1/2} \exp[-x^2/(4D\Delta t)],$$

where x is the displacement in time Δt and D is the self-diffusion coefficient. A constant linear field gradient $G=dH_z/dx$ shall be assumed along the x direction, and spin precession takes place about the z axis. The change in Larmor frequency in time Δt is $\delta-\delta_0=x\gamma G$, so that

$$P(\delta,\Delta t;\delta_0) = (4\pi k\Delta t)^{-1/2} \exp\{-(\delta-\delta_0)^2/(4k\Delta t)\}, \quad \text{(A1)}$$

where $k=(\gamma G)^2 D$.

[26] A. G. Redfield (private communication).

In comparison with Eq. (1), we let the stationary distribution $P(\delta_0)$ be a constant here, namely, unity. For a short time Δt a molecule will not diffuse very far ($\sim 10^{-3}$ cm/sec for H_2O). The actual form of $P(\delta_0)$ is therefore not very important since δ_0 hardly changes in a measurement. In gases or superfluids with large D, this assumption breaks down. The explicit form of $P(\delta_0)$, determined by external field inhomogeneity and the sample shape, must then be used, and $P(\delta,\Delta t;\delta_0)$ should include any dependance upon reflecting barriers, such as the walls of the container which holds the spin sample.

The diffusion decay law for the echo envelope in liquids is obtained by the same procedure applied in obtaining Eq. (26), except that (A1) replaces Eq. (16) with $t\rightarrow\Delta t$ and $P(\delta_0)\approx 1$. For a 90°–180° pulse sequence the echo decay function which determines the lifetime of the echo maximum at $t=2\tau$, or $L=2K$, is given by

$$E_{\max}(2\tau)\sim\exp\{-k[2(\Delta t)^3\sum_{j=1}^{K} j^2 - 2(\Delta t)^2\tau\sum_{j=1}^{K} j+K\Delta t\tau^2]\}.$$

For K large and $K\Delta t=\tau$,

$$E_{\max}(2\tau)\sim\exp\{-(2/3)k\tau^3\}. \qquad \text{(A2)}$$

Let a third 180° pulse be applied at time $t=T$ for $T>2\tau$, and consider the image echo[9] which occurs at $t=2T-2\tau$. Therefore

$$E_{\max}(2T-2\tau)\sim\exp\{-k[(\Delta t)^3\sum_{j=1}^{K} j^2 + \Delta t\sum_{j=1}^{L-K}(j\Delta t-\tau)^2+\Delta t\sum_{j=1}^{M-L}(j\Delta t-T+2\tau)^2]\}, \qquad \text{(A3)}$$

where

$$K\Delta t=\tau, \quad (L-K)\Delta t=T-\tau,$$

and

$$(M-L)\Delta t=T-2\tau.$$

Upon reduction,

$$E_{\max}(2T-2\tau)\sim\exp\{-(2/3)k[(T-2\tau)^3+\tau^3]\}. \qquad \text{(A4)}$$

In the Carr-Purcell method,[11] after a 90° pulse is applied at $t=\tau$, a succession of 180° pulses is applied at $t=3\tau$, 5τ, 7τ, $\cdots$, $S\tau$. The 180° pulses may be numbered from 1 to n. Then we can extend Eq. (A3) above to apply to this case by writing the amplitude of the echo following the Sth 180° pulse as

$$E_{\max}[\tau(S+1)]\sim\exp\{-k[(\Delta t)^3\sum_{j=1}^{K} j^2 + (n-1)(\Delta t)\sum_{j=1}^{2K}(j\Delta t-\tau)^2+\Delta t\sum_{j=1}^{K}(j\Delta t-\tau)^2]\}. \qquad \text{(A5)}$$

The last two summations combine to cancel the term independent of n in the second summation. Therefore (A5) reduces to

$$E_{\max}[\tau(S+1)]\sim\exp\{-kt^3/(12n^2)\}, \qquad \text{(A6)}$$

where $t=2n\tau$ and $K\Delta t=\tau$. (A6) is in agreement with the result obtained by Carr and Purcell, and shows how the attentuation due to diffusion is reduced by the refocussing effect of many 180° pulses.

Now instead of applying a 90°–180°–180° three pulse sequence, let three pulses with arbitrary rotations θ_1–θ_2–θ_3 be applied. In addition to the image echo formed at $t=2T-2\tau$, the unusual stimulated echo[9] is formed at $t=T+\tau$, proportional in amplitude to $\sin\theta_1\sin\theta_2\sin\theta_3$. We will not discuss other echoes formed at $2T$ and $2T-\tau$, which are of the same type as the one at 2τ. Calculation of diffusion attenuation of the echo at $t=T+\tau$ requires our averaging method to be applied to the function $[\cos\delta(t)t]_a[\cos\delta(t)t]_b$. The term $[\cos\delta(t)t]_a$ is to be averaged first in the interval $0\leqslant t\leqslant\tau$ using Eq. (A1). In the interval $\tau\leqslant t\leqslant T$, the term $[\cos\delta(t)\tau]_a$ describes the spectrum of spin magnetism along the z axis, with $\delta(t)$ a diffusing variable. Therefore only a single integration is necessary in the interval $\tau\leqslant t\leqslant T$, using (A1), with Δt replaced by $T-\tau$. The term $[\cos\delta(t)t]_b$ applies to free precession in the interval $T\leqslant t\leqslant T+\tau$ after the third pulse at T, and has the same average as $[\cos\delta(t)t]_a$ in the interval $0\leqslant t\leqslant\tau$. These operations give[9]

$$E_{\max}(T+\tau)\sim\exp\{-k[(2/3)\tau^2+(T-\tau)\tau^2]\}. \qquad \text{(A7)}$$

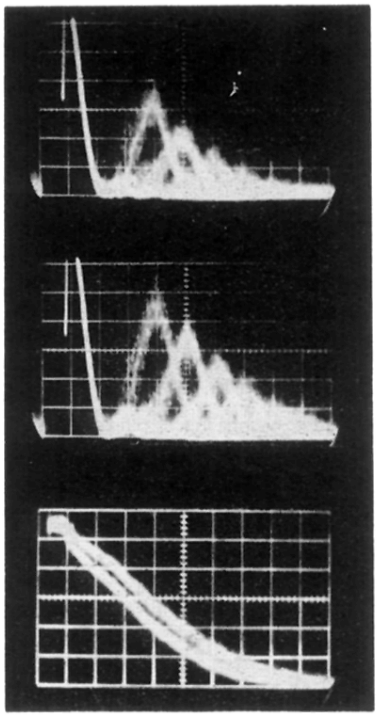

FIG. 11. Zero external magnetic field double resonance of protons in *p*-dichlorobenzene as it affects the free precession of Cl^{35}. The upper trace of the chlorine echo envelope is given for no double resonance ($H_2=0$). Assuming an $\exp[-(t/T_2')^2]$ echo envelope lifetime dependence, $T_2'=0.95$ msec. In the middle oscillographic trace all the conditions are the same except that protons are subjected to double resonance at 11.6 kc/sec with $H_2=2.3$ gauss. T_2' increases to 1.11 msec. The sweep speed for these two traces is 220 μsec/cm division. The lower traces indicate the free precession chlorine signal after the first pulse. A double exposure indicates first an induction signal lifetime of $T_2=0.3$ msec for $H_2=0$ gauss and then a lifetime $T_2=0.4$ msec for $H_2=2.3$ gauss.

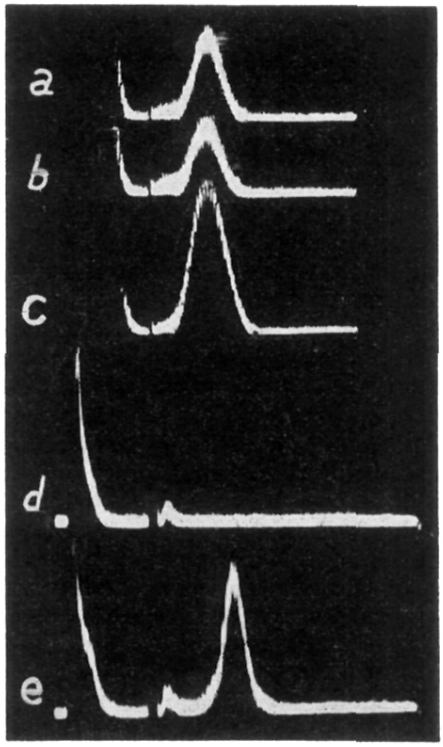

FIG. 5. Oscilloscopic displays of double resonance effect upon Cl^{35} echo amplitude. Trace *a* shows the normal echo ($H_2=0$) in $NaClO_3$ with $2\tau=2.25$ msec and $H_0=25$ gauss along lattice cell edge. Traces *b* and *c* display amplitude changes due to Na^{23} resonance at 395.1 kc/sec (*X* resonance) for $H_2=0.3$ g and 1.0 g, respectively. Trace *d* shows the echo in $p-C_6H_4Cl_2$ completely attenuated at $2\tau=3.4$ msec with $H_0=19.9$ g. Resonance of a portion of the proton spectrum with $H_2=6.7$ g at 88.9 kc/sec in *e* lengthens the echo lifetime radically.